PRIORITY DOCUMENT
SUBMITTED OR TRANSMITTED IN COMPLIANCE WITH RULE 17.1(a) OR (b)

Patent Office
Canberra

I, JULIE BILLINGSLEY, TEAM LEADER EXAMINATION SUPPORT AND SALES hereby certify that annexed is a true copy of the Provisional specification in connection with Application No. 2002950015 for a patent by THE UNIVERSITY OF SYDNEY as filed on 05 July 2002.

WITNESS my hand this
Sixteenth day of July 2003

J. Billingsley

JULIE BILLINGSLEY
TEAM LEADER EXAMINATION
SUPPORT AND SALES

AUSTRALIA

Patents Act 1990

PROVISIONAL SPECIFICATION

Applicants:

THE UNIVERSITY OF SYDNEY

Invention Title:

ANOMALOUS EXPANSION MATERIALS

The invention is described in the following statement:

ANOMALOUS EXPANSION MATERIALS

Field of the Invention

The present invention relates to a method for controlling the thermal expansion behaviour of a material. The term "anomalous" is used herein to define material expansion which is other than expected, such anomalous expansion including negative, zero or even positive expansion behaviour.

Background to the Invention

A vast majority of materials expand when heated. This behaviour is typical (as opposed to anomalous) and is often undesirable in many technological fields. For example, in the field of optics, a relatively small increase in the volume of mirror and other optical device supports can cause large changes in critical performance parameters, such as focal lengths or diffraction widths.

A limited number of known tungstate, molybdate and vanadophosphate compounds display negative thermal expansion (NTE) behaviour. Examples are disclosed in US patents 5,322,559; 5,433,778; 5,514,360; 5,919,720; 6,183,716; 6,187,700; 6,209,352; 6,258,743; in WO 00/64827; in EP 995,723; in JP 63-201034 and in JP 02-208256. Other materials known to display some type of NTE behaviour include beta-quartz, beta-eukryptite and silver iodide.

However, various problems have been identified with a number of these materials. For example, the extent of negative expansion is small, limiting their applications. Also, a number need to be synthesised at prohibitively high temperatures. Also, very few if any possess positive physical characteristics such as optical transparency, low

density, stability, machinability, crystallinity etc. In addition, many are generally not usable in composites because, to avoid formation of cracks or defects in the composites, it is desirable for the degree of contraction to be equal in all directions (isotropic negative expansion), and for negative expansion behaviour to be exhibited over a large temperature range.

In a publication in the Journal of Solid State Chemistry **134**, 164-169 (1997), Williams et al. investigate the disordered crystal structures of $Zn(CN)_2$ and $Ga(CN)_3$. They identify negative thermal expansion in $Zn(CN)_2$ by way of identifying the crystal structure at two separate temperatures but do not demonstrate the continuity of the expansion behaviour, nor identify any general characteristic or understanding of expansion behaviour in that material.

The present inventors, on the other hand, verified negative thermal expansion (NTE) in $Zn(CN)_2$ and surprisingly discovered that the NTE behaviour was continuous, monotonic and nearly linear over a large temperature range. Having identified this, the inventors surprisingly discovered that the NTE behaviour could be attributed to thermal motion of the CN bridges by correlating the extent of NTE to the behaviour of the thermal parameters of the CN bridge. Having then identified this, the inventors discovered that this thermal motion of the CN bridges could be interpreted in terms of vibrational modes, and in turn, phonon modes.

Two different types of transverse vibrational modes were discovered in M-CN-M' containing components. The first (referred to hereafter as "δ_1") involved the displacement of the entire CN bridge away from the M-M' axis in such a way that both the C and N atoms moved in

the same direction. The second (hereafter referred to as "δ_2") involved, in effect, a rotation of the CN bridge about an axis perpendicular to the central M-M' axis, causing the C and N atoms to move in opposite directions. The inventors also discovered that these vibrational modes were consistent with the rigid unit theory of phonon modes.

The inventors further discovered that this analysis implied that the transverse vibrational modes of diatomic (and optionally polyatomic) bridges impacted significantly on the distance between two atoms A and B joined by that bridge.

Summary of the Invention

Accordingly, in a first aspect, the present invention provides a method for controlling the thermal expansion behaviour of a material comprising the step of incorporating into the material a component including one or more diatomic bridges, the or each bridge extending between two atoms in the component, characterised in that the or each diatomic bridge has at least one vibrational mode that causes the two atoms on either side of the bridge to be moved together to a greater extent than competing vibrational mode(s) that cause the two atoms on either side of the bridge to be moved apart.

The component may comprise a portion or the entirety of the material. Preferably the component comprises a portion of the material in an amount or manner that predetermines the material thermal expansion behaviour.

Preferably the component exhibits δ_1- and/or δ_2-like vibrational modes (as defined above) inducing component negative thermal expansion behaviour. Typically the population of the δ_1- and/or δ_2-like vibrational modes

increases when the material is heated, although radiation (eg. infra-red radiation) or another energy source may also have the same effect.

Optionally, anomalous thermal expansion behaviour can occur in some cyanide-containing materials (eg. $Zn[Au(CN)_2]_2$) which arises not only from the δ_1- and/or δ_2-like vibrational effects, but from lattice effects. In this regard, typically such materials include a plurality of diatomic bridges throughout an infinite molecular coordination network defining a lattice structure, whereby changes in lattice geometry can induce eg. material negative thermal expansion behaviour. Typically heating of these materials causes the geometry of the lattice itself to change, often resulting in uniaxial or anisotropic NTE. In addition to these effects, other causes of NTE can include phase transitions, magnetic and electronic transitions and other (not necessarily CN-based) RUMs or phonon modes.

Preferably the diatomic bridge is linear. Negative thermal expansion is typically optimised when the diatomic bridge is linear. In this regard, it is most preferred that the diatomic bridge is a linear cyanide -(CN)- bridge, however, non-linear cyanide or other diatomic bridges may be employed. Other diatomic bridges which may be employed in the method include a carbon monoxide -(CO)- bridge, a di-nitrogen -(NN)- bridge, a nitrogen monoxide -(NO)- bridge, and possibly even a carbide -(CC)- bridge etc.

As defined above, the diatomic bridge extends between two atoms. Preferably these atoms are metals or semi-metals but they may also be non-metals, and combinations thereof.

When a cyanide ion is coordinated to a metal or semi-metal atom, it is preferable that the metal atom coordinates one or more other cyanide ions, which in turn bridge to other atoms.

However, each atom may also coordinate other ligands. These ligands may be uni- or multi-dentate, including but not limited to water, alcohols, diols, thiols, oxalate, nitrate, nitrite, sulfate, phosphate, oxide, sulfide, thiocyanate, non-bridging cyanide, cyanate, nitrogen monoxide, carbon monoxide, dinitrogen etc. Thus, the component can form part of or be defined in a salt. This salt may also be desolvated (usually by heating the salt to drive off the solvent). In this regard, in desolvated salts, it is also not necessary for all coordination sites of the metal atom to be satisfied by a coordinating ligand.

Where the atoms coordinate with other ligands, the component may form part of an assembly that is neutrally, positively or negatively charged. The assembly can, for example, comprise a rigid connected part of the material. When the assembly carries a charge, counter-ions may be incorporated within cavities or pores within the assembly to provide neutrally charged materials. These counter-ions may themselves influence the thermal behaviour of the material, and may also act to influence the expansion behaviour of the material as a whole (eg. by counteracting negative expansion).

The inclusion of counter-ions into the assembly or pores thereof can also confer on the material the ability to exhibit a tuned expansion where eg. the ability to tune the expansion properties arises from ion exchange. In this regard, such tuned expansion can be performed in-situ or by varying preparative conditions. Preferably the counter-

ions are varied either by ion exchange or synthetic modification, to vary the thermal behaviour of the material.

The assembly may also include guest molecules in interstitial cavities within a lattice thereof. A number of different types of guest molecules may be incorporated into the assembly. The guest molecules may also confer on the material the ability to exhibit tuned expansion, where the ability to tune the expansion properties in this case arises from solvent exchange and/or solvent sorption and desorption. Again, such tuned expansion can be performed in-situ or by varying preparative conditions. In this regard preferably the guest molecules influence the thermal behaviour and optionally counteract negative expansion behaviour of the material. When the material is porous the guest molecules can be located in pores of the material. Preferably the guest molecules are varied either by sorption/desorption or synthetic modification, to vary the thermal behaviour of the material.

The inventors have observed that the number of possible topologies of such materials are essentially limitless. The inventors have further observed that the topology of a particular material can be determined to some extent by the number of diatomic bridges (eg. cyanide ions) coordinated to each metal centre, and the geometry of this coordination. For example, the topology may be based on a diamond-, wurzite-, quartz-, cubic-, (4,4)-, (6,3)-, (10,3)-, PtS-, NbO-, Ge_3N_4-, $ThSiO_2$- or PtO_x-type net. The material may comprise more than one interpenetrating net, and these nets may or may not be of the same topology.

The number, topology and size of interpenetrating nets may also affect the solvent or ion accessible volume

of the material. The material may also contain zero-dimensional bridged moieties, such as CN bridged molecular squares.

In a second aspect, the present invention provides a method for controlling the thermal expansion behaviour of a material comprising the step of incorporating into the material a component including one or more multi-atomic bridges, the or each bridge extending between two atoms in the material, characterised in that the or each multi-atomic bridge has at least one vibrational mode that causes the two atoms on either side of the bridge to be moved together to a greater extent than competing vibrational mode(s) that cause the two atoms on either side of the bridge to be moved apart.

In the second aspect both di- and poly-atomic bridges can be employed, for example the di-atomic bridges as defined for the first aspect of the invention, and polyatomic bridges such as cyanamide, dicyanamide, tricyanomethanide, thiocyanate, selenocyanate, cyanate, isothiocyanate, isoselenocyanate, isocyanate, azide, cyanogen and butadyinide. Otherwise, the second aspect is as defined for the first aspect of the invention.

In a third aspect, the present invention provides a composite including a material of the first and second aspects.

The composite of the third aspect may include two or more different materials of the first and second aspects, or a material of the first and second aspects together with a material that does not include a multi-atomic bridge as defined above (hereafter "unrelated material"). In this regard, the composite may further include a binding agent to bind together the different materials, or the material and unrelated material.

The composite may be tuned (eg. by incorporating therein in a predetermined amount or manner a negative thermal expansion component) with the result that the composite, as a whole, displays negative, zero or positive expansion behaviour.

Brief Description of the Drawings

Notwithstanding any other forms which may fall within the scope of the present invention, preferred forms of the invention will now be described, by way of example and with reference to the accompanying drawings in which:

Figure 1 shows a schematic representation of a basic structural unit of the $Zn_xCd_{1-x}(CN)_2$ family;

Figure 2 shows a schematic representation of two interpenetrating diamond-type networks present in the $Zn_xCd_{1-x}(CN)_2$ structural family;

Figures 3(a) to 3(c) show three graphs of temperature versus relative change in unit cell volume for three respective members of the $Zn_xCd_{1-x}(CN)_2$ family;

Figure 4 shows a representation of the basic structural unit present in $Zn^{II}[M^{I}(CN)_2]_2$ (where M = Ag; Au);

Figure 5 shows a representation of one of the six interpenetrating beta quartz-type networks present in the structure of $Zn^{II}[M^{I}(CN)_2]_2$ (where M = Ag; Au);

Figures 6(a) and (b) show two graphs of the thermal expansion behaviour of two respective members of the $Zn^{II}[M^{I}(CN)_2]_2$ family (where M = Ag; Au);

Figure 7 shows a representation of the basic structural unit in the $KCd^{II}[M^{I}(CN)_2]_3$ family (where M = Ag; Au);

Figure 8 shows a representation of one of the distorted cubic nets present in the structure of the $KCd^{II}[M^{I}(CN)_2]_3$ family;

Figures 9(a) and 9(b) show two graphs of the thermal expansion of two respective members of the $KCd^{II}[M^{I}(CN)_2]$ family (where M = Ag; Au);

Figure 10 shows a representation of the basic structural element of $[NMe_4][Cu^{I}Zn^{II}(CN)_4]$;

Figure 11 shows a representation of the diamond-type network present in $[NMe_4][Cu^{I}Zn^{II}(CN)_4]$;

Figure 12 shows a representation of the tetramethylammonium-filled adamantanoid cavities present in the structure of $[NMe_4][Cu^{I}Zn^{II}(CN)_4]$;

Figure 13 shows a graph of the thermal expansion behaviour of $[NMe_4][Cu^{I}Zn^{II}(CN)_4]$;

Figure 14 shows a representation of one of the 'square grids' present in the structure of $Cd^{II}Ni^{II}(CN)_4.xH_2O$;

Figure 15 shows a representation of the structure of $Cd^{II}Ni^{II}(CN)_4.xH_2O$, showing the stacking of cyanide-bridged square grids with alternating cadmium and nickel centres;

Figure 16 shows a representation of the basic structural unit present in $Cd^{II}Pt^{II}(CN)_4$;

Figure 17 shows a representation of the crystal structure of $Cd^{II}Pt^{II}(CN)_4.xH_2O$;

Figures 18(a) and 18(b) show two graphs of the thermal expansion behaviour of two respective members of the $Cd^{II}M^{II}(CN)_4.xH_2O$ family (where M = Ni; Pt);

Figure 19 shows representations of the two transverse vibrational modes present in $Zn(CN)_2$ (and similar systems with linear M-CN-M' linkages);

Figure 20 shows two of the rigid unit modes (RUMs) present in $Zn(CN)_2$, where the zinc coordination spheres are depicted as the tetrahedra, and the cyanide linkages as the joining rods between the tetrahedra; and

Figure 21 shows the variation of thermal parameters of atoms in $Zn(CN)_2$ as determined by single crystal X-ray diffraction.

Modes for Carrying Out the Invention

Prior to describing the present invention in detail, further background on how the present inventors arrived at the present invention is provided.

The inventors first observed that in the above described prior art materials, negative thermal expansion (NTE) arose from vibrations of a single O-atom bridge. In this regard, both ZrW_2O_8 and $Sc_2W_3O_{12}$ (disclosed in the above referenced patents) were noted to be examples of oxide-bridged NTE compounds, in which NTE properties arose from thermally induced vibrations of the oxide bridge.

In these compounds, two atoms (M and M´, for example) are connected by an O atom. As the material is heated, this M-O-M´ link vibrates such that the O atom moves perpendicularly to the M-M´ axis, causing a contraction in the material.

However, from crystallographic studies, the present inventors surprisingly discovered negative expansion behaviour in certain two-atom (or diatomic) bridges and surmised that this negative expansion might also occur in some multi-atomic (ie. greater than two atom) bridges.

More particularly, the inventors observed that the thermal parameters with cyanide diatomic bridges were increasing with temperature much more quickly than those of the metal atoms to which they were joined. In this regard, reference is made to Figure 21 which depicts the variation of the thermal parameters of atoms in $Zn(CN)_2$ as determined by single crystal X-ray diffraction. The thermal parameters of the CN bridge normal to the M-CN-M´

axis can be easily seen to increase significantly more rapidly with increasing temperature than other thermal parameters.

This analysis enabled the inventors to characterise the mechanism of negative expansion in the cyanide -(CN)- bridge. In particular, whilst the inventors discovered that the diatomic bridge could vibrate like the O-bridged NTE materials described above, they surprisingly discovered new vibrational modes in the diatomic bridge. These included the δ_1 and δ_2 vibrational modes (defined above) which, when thermally populated, contributed to negative expansion in materials incorporating these bridges. They also discovered materials in which lattice effects as well as NTE vibrational modes contributed to the anomalous thermal expansion behaviour, leading to the discovery and characterisation of a whole host of new materials with varying expansion properties.

They further discovered that, depending on the proportion, distribution and type of diatomic bridges in a given material, anomalous expansion behaviour resulted, namely negative thermal expansion (NTE), zero thermal expansion (ZTE) or positive thermal expansion (PTE). By controlling the proportion, distribution, type of diatomic bridge and the atoms being bridged, the inventors obtained tunable thermal expansion (TTE).

Preferred materials according to the present invention were then able to be formulated to include one or more A-CN-B components (where A and B were the same or different atom, preferably a metal or semi-metal, but also a non-metal, and combinations thereof). Other diatomic bridges included carbon monoxide A-CO-B, di-nitrogen A-NN-B, nitrogen monoxide A-NO-B, and carbide A-CC-B.

The thermal expansion behaviour of materials was quantified by the coefficient of thermal expansion α_l, defined as the relative change in length per unit temperature change. Typically observed expansion values of α_l for common materials were noted to be of the order of 1 to 50 x 10^{-6} K^{-1}.

Prior to the present invention, the most pronounced isotropic NTE behaviour over a significant temperature range was reported for ZrW_2O_8, a compound whose coefficient of thermal expansion was around -9 x 10^{-6} K^{-1}. Of the materials that display anisotropic NTE, $Sc_2W_3O_{12}$ displayed the most pronounced NTE effect in one direction over a significant temperature range, with a coefficient of thermal expansion of -11 x 10^{-6} K^{-1}.

Preferred Embodiments of the Present Invention.

Methods for controlling the thermal expansion behaviour of solid materials were investigated with a range of solid materials. The methods were observed to significantly enhance the anomalous expansion behaviour of these solid materials over prior art expansion materials (especially in the degree of negative expansion). Initial experiments focussed on cyanide ion bridges.

Cyanide-bridged negative expansion components were observed to have a number of advantages over current NTE materials including:

- The extent of negative expansion was observed to be much larger than ever before observed. For example, $Cd(CN)_2$ exhibited isotropic NTE with a coefficient of thermal expansion of -21 x 10^{-6} K^{-1} and $Zn[Au(CN)_2]_2$ exhibited anisotropic NTE with a coefficient of thermal expansion in one direction of -50 x 10^{-6} K^{-1};

- The synthesis of materials including a cyanide-bridged component was considerably simpler than the prior art NTE materials.
- Many of the materials according to the invention were able to be synthesised using conventional solvents (such as water), at room temperature, and without specialist equipment, and the starting materials were often low cost and readily available;
- In many cases, the thermal expansion properties of the materials were able to be tuned by selective doping of metal sites, modification of guest molecules, modification of counter-ions, and degree of interpenetration of material topology;
- For example, the materials were able to be doped with trace elements such as erbium and used in optical fibres, or in lasers, where controlled thermal expansion properties are highly desirable;
- The materials were also able to be applied as bobbins for superconducting coils, in optical devices, in thermal transfer devices and in zero insertion-force sockets.
- Many of the materials were able to be grown as large single crystals and to be optically transparent;
- Some of the materials also enabled the formation of single crystal products containing coefficient of thermal expansion gradients within each crystal, rendering the materials useful in thermal electronics etc;
- The negative expansion substances and materials were also able to be incorporated into or formulated as part of other materials to alter the expansion behaviour of those other materials, ie. rendering them net negative, zero or positive expansion materials.

Thus, the methods of the present invention were able to provide materials having predetermined NTE, ZTE, PTE and TTE behaviour.

TTE was applied to materials requiring PTE compensation, and to produce materials displaying particular thermal expansion behaviours. Compensation for PTE was noted to be of particular importance in the communications industry, for example, where changes in the size of optical diffraction gratings were observed to limit data quality and quantity.

These far-reaching improvements rendered the materials produced according to the invention of significant potential application wherever controlled expansion materials were required.

Various materials developed by the inventors including cyanide diatomic bridges will now be described, including their synthesis and characterisation. The following materials were observed to be constituted typically, though not always, by "infinite" molecular coordination networks (for example, where the diatomic bridge is present throughout the material). Further, composites including two or more of these materials (or one of these materials and an unrelated material) were produced.

Material Examples:

(a) Materials based on the $Zn(CN)_2$-type or 2x(6,4) cubic structure (doubly interpenetrating diamond-type nets). Variations included substitution of divalent metals for some or all of the Zn atoms. Such divalent metal ions included Cd(II), Hg(II), Mn(II), Be(II), Mg(II), Pb(II) and Co(II). Variations also included substitution of mixtures of univalent, divalent and trivalent metal ions for Zn to give materials of the form:

$\{(M1_1^{II})_{x1}(M1_2^{II})_{x2}\ldots(M1_n^{II})_{xn}\}\{(M2_1^{I})(M3_1^{III})\}_{y1}\{(M2_2^{I})(M3_2^{III})\}_{y2}\ldots\{(M2_n^{I})(M3_n^{III})\}_{ym}(CN)_2$ where $M1_i$ included Zn(II), Cd(II), Hg(II), Mn(II), Be(II), Mg(II), Pb(II) and Co(II); $M2_j$ included Li(I) and Cu(I); $M3_k$ included Al(III), Ga(III) and In(III); n and m being any non-negative whole numbers with at least one greater than or equal to unity; and (x1 + x2 +... +xn) + 2 x (y1 + y2 +... +ym) = 1. Examples of this class included $Zn(CN)_2$, $Zn_{0.8}Cd_{0.2}(CN)_2$, $Cd(CN)_2$, $Mn(CN)_2$, $Zn_{0.5}Hg_{0.5}(CN)_2$, $Li_{0.5}Ga_{0.5}(CN)_2$ and $Cu_{0.5}Al_{0.5}(CN)_2$.

(b) Materials of the general formula given in (a) above but with a single diamond-type network rather than two interpenetrating networks, optionally with counterions or molecules incorporated into the structure. Incorporation of counterions into the interstitial cavities required an appropriate inclusion of lower- or higher-valent metals into the network lattice. Examples of this class included $Cd(CN)_2.\frac{1}{2}CCl_4$, $[NMe_4]_{0.5}[Cu^{I}_{0.5}Zn^{II}_{0.5}(CN)_2]$, $Cd(CN)_2.CMe_4$, $Cd(CN)_2.CMe_3Cl$, $Cd(CN)_2.CMe_2Cl_2$, $Cd(CN)_2.CMeCl_3$, $Cd(CN)_2.CCl_4$, $Cd_{0.5}Hg_{0.5}(CN)_2.CCl_4$, $Cd_{0.5}Zn_{0.5}(CN)_2.CCl_4$.

(c) Materials of the general formula given in (a) and (b) above but with more than two interpenetrating diamond-type networks.

(d) Materials based on the $Ga(CN)_3$-type cubic structure. Some such materials satisfied the general formula $\{(M1_1^{III})_{x1}(M1_2^{III})_{x2}\ldots(M1_n^{III})_{xn}\}\{(M2_1^{II})(M3_1^{IV})\}_{y1}\{(M2_2^{II})(M3_2^{IV})\}_{y2}\ldots\{(M2_m^{II})(M3_m^{IV})\}_{ym}(CN)_3$ where M1 included trivalent metal ions such as Fe(III), Co(III), Cr(III), Ti(III), Al(III), Ir(III), Ga(III), In(III) and Sc(III); M2 included divalent metal ions such as Mg(II), Zn(II), Cd(II), Co(II), Fe(II), Ru(II), Mn(II) and Ni(II); M3 included tetravalent metal ions such as Pd(IV) and Pt(IV); n and m being non-negative whole numbers with at least one greater than or equal to unity; and (x1 + x2 +... +xn) + 2 x (y1 +

y2 + ... + ym) = 1. Examples of this class included $Ga^{III}(CN)_3$, $Co^{III}(CN)_3$, $Al^{III}(CN)_3$ and $Cd^{II}_{0.5}Pt^{IV}_{0.5}(CN)_3$.

(e) Materials of the general formula given in (d) above but with other ions or molecules being incorporated into the structure. Incorporation of ions into the interstitial cavities required an appropriate inclusion of lower- or higher-valent metals into the network lattice. Examples of this class included the known Prussian blues compounds (e.g., $K[Fe^{II}Fe^{III}(CN)_6].xH_2O$) and their analogues.

(f) Materials of the types described in (d) and (e) above but with more than one interpenetrating cubic framework.

(g) Other simple metal cyanides not explicitly belonging to classes (a) to (f) above of the general form $(M1^{n1+})_{x1}(M2^{n2+})_{x2}...(Mk^{nk+})_{xk}(CN)_i(.\{guest\})$ where M1, M2 ... Mk were metals with oxidation states n1+, n2+ ... nk+ respectively; k and i were positive whole numbers; (x1 x n1) + (x2 x n2) + ... + (xk x nk) = i; and {guest}, when present, included any solvent or molecular species such as water, alcohols, organic solvents or gas molecules. Such materials optionally consisted single or multiple interpenetrating regular nets, such as the quartz, NbO, PtS, Ge_3N_4, (10,3), $ThSiO_2$, PtO_x or wurtzite nets. Examples included $Ag^{I}CN$, $Au^{I}CN$, $Zn^{II}Ag^{I}_2(CN)_4$ and $Zn^{II}Au^{I}_2(CN)_4$.

(h) Materials of the general formula given in (g) above but with other ions or molecules incorporated into the structure. Incorporation of ions into the interstitial cavities required an appropriate inclusion of lower- or higher-valent metals into the network lattice. Examples included $KCd^{II}[Ag^{I}(CN)_2]_3$ and $KCd^{II}[Au^{I}(CN)_2]_3$

(i) Other materials not explicitly belonging to classes (a) to (g) above that contained cyanide-bridged atoms. Included were cyanide-bridged materials in which the coordination spheres of some or all metal atoms included

one or more non-cyanide bridges, such as water, alcohols, diols, thiols, oxalate, nitrate, nitrite, sulfate, phosphate, oxide, sulfide, thiocyanate, (non-bridging) cyanide, cyanate, nitrogen monoxide, carbon monoxide or dinitrogen. Such materials optionally consisted of regular nets, and optionally included interstitial ions or guest molecules. Examples included $Ni^{II}(CN)_2.xH_2O$, $Fe_4[Re_6Se_8(CN)_6]_3.36H_2O$, $Cd^{II}Ni^{II}(CN)_4.xH_2O$ and $Cd^{II}Pt^{II}(CN)_4.xH_2O$.

(j) Materials of the type described in (i) above that contained finite cyanide-bridged species. Such materials optionally contained cyanide-bridged polyhedra, polygons or finite chains. The cyanide-containing species optionally contained branches. Such materials also optionally contained components unrelated or unconnected to the cyanide-bridged moieties.

(k) Materials of the type described in (a) to (i) above where chemical composition varied within the one crystal/crystallite, as was achieved by variation of crystallisation conditions such as concentrations and temperatures during crystallisation. Examples included $Zn_xCd_{1-x}(CN)_2$.

(l) Amorphous materials or glasses based on any of the systems defined in (a) to (k) above.

Preparations of these materials required a source of cyanide ions. Such sources included simple cyanide salts or their solutions, polycyanometallate salts or their solutions, cyanide precursors such as trimethylsilyl cyanide, organic nitriles, isocyanide salts or their solutions, organic isonitriles, hydrogen cyanide gas or its solutions, cyanohydrins or their solutions or any other cyanide-containing solid-, liquid-, gaseous- or solution-phase reagents. Materials were then prepared by a number of methods, including:

(a) Slow diffusion of solutions containing the appropriate metal ions, any other coordinated ligands and a source of cyanide ions;

(b) Diffusion of reagents through thin films, gels or capillaries;

(c) Hydrothermal, solvothermal, and other high-temperature preparations;

(d) Solid-phase reactions, which optionally employed high temperatures and high pressures;

(e) Direct combination of reagents and isolation of products by techniques including precipitation and filtration, evaporation, crystallisation, sublimation and vapour deposition;

(f) Passage of hydrogen cyanide gas (or other gaseous cyanide-precursor) through solutions containing appropriate metal ions, ligands and guest molecules.

(g) Decomposition or reaction of precursor compounds, in which volatile or reactive components of the precursor were removed or reacted.

Preferred materials according to the present invention had a number of features that made them suitable for physical application, including their facile synthesis, ready availability and unprecedented NTE and TTE behaviours. Further physical applications of materials containing cyanide-bridged atoms included:

(a) Substrates designed to exhibit a specific thermal expansion behaviour; for example, to exhibit ZTE or to match that of another component, such as silicon. Such materials find use in electronics as circuit boards or silicon supports; as optical components or supports; as housing or substrates for optical diffraction gratings such as Bragg diffraction gratings in optical fibres;

(b) Components in composite materials where the thermal expansion properties of the cyanide-containing component are used to compensate for the thermal expansion property of the remaining component. As for (a) above, such compensation may be needed to provide a composite material with a specific thermal expansion behaviour. The applications of these composites were similar to those listed in (a) above;

(c) Composites capable of directing heat flow through the presence of coefficient of thermal expansion gradients in single-crystalline samples. Such composites may form a basis for thermal circuitry, acting as thermal diodes;

(d) Optical devices including optical fibres and lasers; and

(e) Zero-insertion force sockets.

Several materials containing cyanide-bridged atoms were characterised structurally. Their thermal expansion properties were also monitored by structural investigation. It was noted that a large and diverse family of materials exhibiting a range of useful thermal expansion properties and containing the same basic structural motif of cyanide-bridged atoms could be synthesised. Notable differences between all five types of characterised materials supported this understanding.

Materials with different degrees of interpenetration, topology, guest inclusion, charge, chemical composition and thermal expansion properties were also discovered. The common feature to each was the NTE component to the overall thermal expansion behaviour derived from the presence of M-CN-M´ linkages. Lattice effects were also noted to play a role in the anomalous thermal expansion properties of some of the compounds (eg those described in Examples 2 and 3 below).

The following non-limiting examples illustrate a diversity of anomalous thermal behaviours possible within cyanide-bridged materials constituted by or including the following compounds:

EXAMPLE 1

Unprecedented degrees of NTE were discovered in simple metal cyanides of the $Zn(CN)_2$ structural family. The structure consisted of two interpenetrating diamond-type networks, with metal atoms acting as tetrahedral four-connectors, and cyanide ions as linear bridges.

Three salts were characterised structurally:

$Zn(CN)_2$ (**A1**);

$Zn_xCd_{1-x}(CN)_2$ (**A2**), where x ~ 0.2 and

$Cd(CN)_2$ (**A3**).

Two neutral diamond-type networks were observed to interpenetrate, each related by translation (see Figures 1 and 2). Further materials were synthesised by further variation of the metal units and, although these salts were not characterised, their similar crystal morphologies suggested the framework structure was retained.

Measured crystallographic details of **A1** were: *cubic*, space group Pn-3m, unit cell *a* = 5.9231(3) Å, V = 207.81(3) Å^3 (150 K); *a* = 5.9142(3) Å, V = 206.87(3) Å^3 (225 K); *a* = 5.9079(3)Å, V = 206.21(3) Å^3 (300 K); *a* = 5.9011(6), V = 205.49(6) Å^3 (375 K).

Measured crystallographic details of **A2** were: *cubic*, space group Pn-3m, unit cell *a* = 6.0010(5) Å, V = 216.10(5) Å^3 (150 K); *a* = 5.9927(4) Å, V = 215.21(3) Å^3 (225 K); *a* = 5.9843(4)Å, V = 214.31(3) Å^3 (300 K); *a* = 5.9782(4), V = 213.65(4) Å^3 (375 K).

Measured crystallographic details of **A3** were: *cubic*, space group Pn-3m , unit cell *a* = 6.325(2) Å, V

= 253.0(3) Å^3 (150 K); *a* = 6.3213(4) Å, V = 252.29(4) Å^3 (225 K); *a* = 6.3022(4) Å, V = 250.31(4) Å^3 (375 K).

A3 was found to undergo reversible structural transitions at temperatures below 150 K which served to enhance the NTE. These transitions involved doubling and quadrupling of the unit cell parameter, with retention of the cubic symmetry.

Figure 1 shows an ORTEP representation of the basic structural unit of the $Zn_xCd_{1-x}(CN)_2$ family, being part of the structure of compounds **A1**, **A2** and **A3**. Metal atoms are designated M and cyanide ions are designated CN. Each metal atom acts as a tetrahedral connector to four cyanide ions (ie. coordinates four cyanide ions in a tetrahedral arrangement). Each cyanide ion acts as a linear connector between two metal atoms. Each metal atom is coordinatively saturated in these compounds. Also, in each structure, the cyanide ion is disordered so that the C and N atoms are crystallographically indistinguishable.

Figure 2 illustrates two interpenetrating diamond-type networks present in the $Zn_xCd_{1-x}(CN)_2$ structural family which are common to the structures of compounds **A1**, **A2** and **A3**. The two identical networks are shaded differently, are completely disjoint and are related to each other by translation and rotation. Each node in this illustration corresponds to a metal centre; the long rods correspond to M-CN-M´ linkages. There is no void volume or inclusion of guests in these compounds.

Figures 3(a), 3(b) and 3(c) show the relative changes in unit cell volumes in each of the three members of the $Zn_xCd_{1-x}(CN)_2$ family. As each compound has cubic symmetry, the contractions indicated by these graphs is equal in all directions, or isotropic. The relative volume change in

$Cd(CN)_2$ is the most pronounced example of isotropic NTE reported to date.

The composition of the structure common to the compounds **A1 - A3** was varied systematically and it was noted that with a potentially limitless number of solid solutions possible, that the thermal expansion properties of these materials were able to be fine-tuned.

EXAMPLE 2

The lattice type, metal oxidation state and coordination preference of **A1 - A3** was varied and enabled the discovery of unprecedented uniaxial NTE in chiral mixed-metal cyanides. The structure of these materials consisted of six interpenetrated beta-quartz-type nets, imparting a hexagonal, rather than cubic symmetry. Two salts were characterised structurally, namely: $Zn^{II}[Ag^{I}(CN)_2]_2$ (**B1**) and $Zn^{II}[Au^{I}(CN)_2]_2$ (**B2**).

Six quartz networks were observed to interpenetrate, each related by translation or rotation. As for quartz, each network was chiral, and each of the six interpenetrated networks in **B1** and **B2** had the same handedness.

Crystallographic details of **B1** were: *hexagonal*, space group $P6_222$, unit cell a = 9.416(6) Å, c = 18.13(1) Å, V = 1392(3) Å^3 (107 K); a = 9.451(3) Å, c = 18.217(5) Å, V = 1409.2(7) Å^3 (200 K).

Crystallographic details of **B2** were: *hexagonal*, space group $P6_222$, unit cell a = 8.435(1) Å, c = 20.785(4) Å, V = 1280.7(6) Å^3 (150 K); a = 8.440(3) Å, c = 20.723(5) Å, V = 1278.2(8) Å^3 (200 K).

Figure 4 is an ORTEP representation of the basic structural unit present in $Zn^{II}[M^{I}(CN)_2]_2$ (where M = Ag; Au),

being part of the structures of **B1** and **B2**. Each zinc atom (designated Zn) acts as a tetrahedral connector to four cyanide ions, being coordinated to the nitrogen atom of the four cyanide ions in a tetrahedral arrangement. Each gold or silver atom (designated M) acts as a slightly bent connector between two cyanide ions, the M atom being coordinated to the carbon atom of two cyanide ions in an approximately linear arrangement. Each cyanide ion (designated CN) acts as an approximately linear connector between a zinc atom and a gold or silver (M) atom.

Figure 5 illustrates one of the six interpenetrating beta-quartz-type networks that occurred in the structures of $Zn^{II}[M^{I}(CN)_2]_2$, (where M = Ag; Au), being part of the structures of **B1** and **B2**. The M atoms are designated M and the zinc atoms are designated Zn. Each of the triangular channels in the representation is in fact a helix. Moreover, each helix has the same handedness, not only within each framework, but within the six frameworks that interpenetrate in the overall structure. Consequently, both materials grow as homochiral crystals and consequently rotate plane polarised light in only one direction.

Figures 6(a) and 6(b) show the relative changes in unit cell parameters that occurred when each $Zn^{II}[M^{I}(CN)_2]_2$ network was heated. The variation of the metal M had significant effect on the thermal expansion properties of the material. Also noted was the large negative change in the relative magnitude of the c-axis in $Zn^{II}[Au^{I}(CN)_2]_2$. This was the most pronounced example of uniaxial NTE reported to date.

As with the materials **A1 - A3**, compositional variation of the metal sites in **B1** and **B2** provided a potentially limitless number of solid solutions with

different thermal expansion properties. The topological difference between **A1** - **A3** and **B1** and **B2** illustrated further the structural variability within simple cyanide-bridged materials.

EXAMPLE 3

Further variation of one of the metal components of **B1** and **B2** enabled the discovery of two new mixed-metal cyanides. These materials exhibited a different topology to that of **B1** and **B2**, comprising three interpenetrating distorted cubic nets. Interstitial cations occupied vacancies between these nets. As observed for **B2**, these compounds exhibited uniaxial NTE.

Two salts were characterised structurally, namely:

$KCd^{II}[Ag^{I}(CN)_2]_3$ (**C1**) and

$KCd^{II}[Au^{I}(CN)_2]_3$ (**C2**).

Three distorted cubic nets interpenetrated, each related by translation or rotation. Vacancies between the nets were occupied by interstitial cations.

Crystallographic details of **C1** were: *hexagonal*, space group P-3 , unit cell a = 6.855(3) Å, c = 8.425(4) Å, V = 342.9(3) Å^3 (107 K); a = 6.900 Å, c = 8.407 Å, V = 346.6 Å^3(200 K).

Crystallographic details of **C2** were: *hexagonal*, space group P-3 , unit cell a = 6.777(3) Å, c = 8.305(5) Å, V = 330.3(3) Å^3 (107 K); a = 6.8052 Å, c = 8.2732 Å, V = 331.81 Å^3(200 K).

Figure 7 shows an ORTEP representation of the basic structural unit in the $KCd^{II}[M^{I}(CN)_2]_3$ family (where M =Ag; Au), being part of the structure of compounds **C1** and **C2**. Each cadmium atom (designated Cd) acts as an octahedral connector to six cyanide ions, being coordinated to the nitrogen atoms of six cyanide ions in an octahedral

arrangement. Each silver or gold atom (designated M) acts as a linear connector between two cyanide ions, being coordinated by the carbon atoms of two cyanide ions. Each cyanide ion acts as a slightly-bent connector between a cadmium atom and a silver or gold atom. Potassium ions lie in interstitial cavities in which they are weakly coordinated by nitrogen atoms of surrounding cyanide ions (not shown in Figure 7).

Figure 8 illustrates one of the three interpenetrating distorted cubic networks that occur in the structure of the $KCd^{II}[M^{I}(CN)_2]_3$ family, being part of the structures of **C1** and **C2**. The three nets interpenetrate, with interstitial cations occupying vacancies generated in the structure. The cadmium atoms (designated Cd) act as octahedral connectors to six M atoms through cyanide bridges. Each M atom (designated M) acts as a linear connector to two cadmium atoms through cyanide bridges.

Figures 9(a) and 9(b) show the thermal expansion behaviour of the family $KCd^{II}[M^{I}(CN)_2]_3$ (where M = Ag; Au), illustrating the relative changes in unit cell parameters that occur in each network when heated. Of particular interest is the theme of NTE along the c-axis. As noticed with the $Zn^{II}M^{I}_2(CN)_4$ family, the extent of NTE is decreased upon replacement of gold atoms by silver atoms.

EXAMPLE 4

The **A**-type structure was varied to produce an anionic network which forced the inclusion of cations rather than a second interpenetrating diamond-type net into the adamantanoid cavities of the diamond-type framework. The presence of large unbound cations led to the discovery of

PTE in this material. One salt was characterised structurally, namely:

$[NMe_4][Cu^{I}Zn^{II}(CN)_4]$ (**D**).

Half of the adamantanoid cavities formed by the single anionic diamond-type network were occupied by tetramethylammonium cations.

Crystallographic details of **D** were: *cubic*, space group F-43m , unit cell a = 11.587(3) Å, V = 1555.5(9) Å^3 (107 K); a = 11.6406(5) Å, V = 1577.3(5) Å^3 (200 K)

Figure 10 is an ORTEP representation of the basic structural element of $[NMe_4][Cu^{I}Zn^{II}(CN)_4]$, being part of the structure of **D**. The zinc and copper atoms (designated Zn and Cu respectively) each act as tetrahedral connectors to four cyanide ions. Each cyanide ion links a copper and a zinc atom in a linear arrangement, with the carbon atom being bound to a copper atom, and the nitrogen being bound to a zinc atom. Further, the cyanide ions are ordered so that each copper atom is bound to the carbon of each of four cyanide ions and each zinc atom binds the nitrogen of four cyanide ions. Overall charge balance is obtained by inclusion of the tetramethylammonium cation, which occupies every second adamantanoid cavity.

This structural unit may be compared to that of $Zn(CN)_2$ (see Figure 1). The topologies are identical, except that the cation inclusion in this compound precludes the interpenetration of a second diamond-type net.

Figure 11 is a representation of the diamond-type network present in $[NMe_4][Cu^{I}Zn^{II}(CN)_4]$, part of the diamond-type network structure of **D**. The tetramethylammonium cations, which occupy some of the channel space, have been removed for clarity. Each node corresponds to a metal atom: Zn designating zinc atoms and Cu designating copper

atoms. The rod-like connectors correspond to M-CN-M´ linkages.

Figure 12 shows representations of the tetramethylammonium-filled adamantanoid cavities present in the structure of $[NMe_4][Cu^{I}Zn^{II}(CN)_4]$, being one of the adamantanoid cavities present in the structure of **D**. Every second such cavity contains a tetramethylammonium cation, and the remainder are vacant. The cation is positioned so that each methyl group points towards one of the four hexagonal (or cyclohexane-like) 'windows' of the cavity.

Figure 13 is a graph of the thermal expansion behaviour of $[NMe_4][Cu^{I}Zn^{II}(CN)_4]$, showing the relative volume change that occurs in compound **D** upon heating. The PTE of this material is in sharp contrast with the NTE exhibited by the parent structure of $Zn(CN)_2$.

EXAMPLE 5

Compounds **A**, **B**, **C** and **D** were further varied, leading to the discovery of new cyanide-bridged compounds in which some of the metals bound ligands other than cyanide, solvent was included and which contained non-linear M-CN-M´ linkages. The materials were observed to exhibit overall PTE and uniaxial ZTE. Two salts were characterised structurally, namely:

$Cd^{II}Ni^{II}(CN)_4.xH_2O$ (**E1**) and

$Cd^{II}Pt^{II}(CN)_4.xH_2O$ (**E2**).

The structure of **E1** comprised stacked cyanide-bridged square grids with solvent water molecules joining subsequent layers. Ni and Cd atoms each acted as square-planar connectors, binding four cyanide ions. They occupied alternate positions in each layer, with each Cd atom coordinating two aquo ligands in an axial arrangement.

The structure of **E2** comprised cyanide-bridged square grids with water molecules joining subsequent layers. Pt and Cd atoms each acted as square-planar connectors, binding four cyanide ions. They occupied alternate positions in each layer, with each Cd atom coordinating two bridging aquo ligands in a *cis*-arrangement.

Further materials were synthesised by further variation of the metal units, and although these salts were not characterised, their similar morphologies suggested that the framework structure was retained.

Crystallographic details of **E1** were: *orthorhombic*, space group Cmcm, unit cell a = 7.440(2) Å, b = 12.216(3) Å, c = 14.253(2) Å, V = 1295.3(4) Å^3 (107 K); a = 7.464(4) Å, b = 12.268(6) Å, c = 14.250(5) Å, V = 1304.8(9) Å^3 (150 K).

Crystallographic details of **E2** were: *orthorhombic*, space group I222, unit cell a = 9.869(3) Å, b = 9.982(3) Å, c = 10.709(2) Å, V = 1054.9(6) Å^3 (107 K); a = 9.927(3) Å, b = 10.039(3) Å, c = 10.703(3) Å, V = 1066.7(8) Å^3 (200 K).

Figure 14 shows an ORTEP representation of one of the 'square grids' present in the structure of $Cd^{II}Ni^{II}(CN)_4.xH_2O$, being part of the structure of **E1**. Each Nickel atom (designated Ni) binds four cyanide ions in a square planar arrangement, being coordinated by the carbon atoms of four cyanide ions in a square planar arrangement. Each cadmium atom (designated Cd) binds four cyanide ions in a square planar arrangement with two water molecules completing its octahedral coordination environment in the axial positions. Each cyanide ion bridges one Ni and one Cd atom in a non-linear fashion. The nitrogen atoms of four cyanide ions occupy four equatorial positions and two water molecules occupy the remaining two axial positions.

This connectivity resulted in two dimensional square grids, in which cadmium and nickel atoms alternated, bridged by cyanide ions. These grids then stacked on top of one another, with solvent water molecules (not illustrated in Figure 14) occupying the space between layers (ie. occupying the interstitial cavities produced by the framework).

Figure 15 shows a representation of the structure of $Cd^{II}Ni^{II}(CN)_4$, illustrating the stacked square grid arrangement in the structure of **E1**. In particular, Figure 15 shows the stacking of cyanide-bridged square grids with alternating cadmium (designated Cd) and nickel (designated Ni) centres. Water molecules (omitted for clarity) occupy the void volume generated between subsequent layers. Each cyanide ion joins a cadmium centre and a nickel centre in a slightly-bent geometry, resulting in the wave-like topology of each sheet.

Figure 16 shows an ORTEP representation of the basic structural unit present in $Cd^{II}Pt^{II}(CN)_4$, being part of the structure of **E2**. Each platinum atom (designated Pt) is coordinated in a square-planar arrangement by the carbon atom of four cyanide ions, and interacts weakly with a neighbouring platinum atom in a direction perpendicular to its coordination plane. Each cadmium atom (designated Cd) binds four cyanide ions in a see-saw arrangement with two bridging water molecules completing its octahedral coordination environment in adjacent positions. In particular, each cadmium centre has an octahedral coordination sphere, with four sites (in a see-saw arrangement) occupied by the nitrogen atom of four cyanide ions, and the remaining two sites occupied by water molecules. These water molecules also bind a nearby cadmium atom, linking adjacent sheets together. Water

molecules (omitted from this diagram) occupy channels or interstitial cavities created in this structure. Each cyanide ion bridges one Pt and one Cd atom; some in a linear fashion, others with a bent geometry.

Figure 17 shows a representation of the crystal structure of $Cd^{II}Pt^{II}(CN)_4.xH_2O$, illustrating the pseudo-cubic arrangement of the structure of **E2**. Square grids comprising alternating cyanide-linked cadmium (designated Cd) and platinum (designated Pt) centres are joined in three dimensions by bridging water molecules. Water molecules (omitted for clarity) occupy the void volume (channels) generated by this structure.

Figures 18(a) and 18(b) graph the thermal expansion behaviour of the $Cd^{II}M^{II}(CN)_4.xH_2O$ family (where M = Ni; Pt), showing the relative changes in unit cell parameters that occur when each compound is heated. Of particular note is the uniaxial ZTE exhibited along the c-axis in both materials.

Examples 1 to 4 illustrate the versatility of thermal expansion properties possible in cyanide-bridged materials. The combination of the NTE effect caused by linear cyanide bridges with the PTE effect of solvent and interstitial ions together with variation of framework topology, degree of interpenetration and composition was observed to impart a subtle and powerful degree of control over the thermal expansion properties of these materials. Other subtle effects, such as cyanide order/disorder and defect inclusion were also observed to affect the thermal expansion properties of these materials.

The extent of NTE exhibited by compounds **A1 - A3**, **B2**, **C1** and **C2** indicated that these materials would find diverse application in industry. However, it was the generality and tunability of the thermal expansion

properties in these compounds that indicated that these compounds would become a highly important class of materials.

Example 6 Compound Synthesis and Characterisation

Synthesis

Single crystals of **A1** and **A2** were prepared by slow diffusion of solutions of zinc(II) acetate into stoichiometric (1:1) solutions of potassium tetracyanozincate(II) (**A1**) or potassium tetracyanocadmate(II) (**A2**). Single crystals of **A3** were prepared by slow evaporation of a saturated solution of cadmium(II) cyanide prepared by mixing aqueous solutions containing stoichiometric amounts of cadmium(II) nitrate and potassium tetracyanocadmate(II).

Alternatively, single crystals of **A1** were prepared by slow diffusion of aqueous solutions of potassium cyanide and zinc(II) acetate in stoichiometric quantities (2:1).

All three compounds were able to be prepared as bulk samples without the need for slow diffusion. Powder diffraction of samples prepared in this way illustrated the high degree of crystallinity of the products.

Many other salts were prepared in these ways, and although they were not structurally characterised, their morphology indicated that they would share the same structure as the compounds **A1**, **A2** and **A3**.

Diffusion techniques mentioned above included the use of:

(a) H-shaped cells, where the reactants diffused toward one another through the horizontal arm of the vessel;

(b) Test tubes, where an aqueous solution of one reagent was layered above an aqueous solution of the other

reagent. Often a buffer region of pure solvent was introduced between the two solutions;

(c) U-shaped tubes, where the reagents diffused toward one another through a curved region beneath the initial position of the solutions.

Large colourless crystals were grown by each of these techniques over time periods ranging from days (test-tubes) and weeks (U-tubes) to months (H-cells).

Structural Characterisation

Single crystals of **A1**, **A2** and **A3** were placed in Lindemann capillaries and transferred to a Bruker-AXS Smart 1000 CCD diffractometer equipped with Mo-K_α graphite monochromated radiation (lambda = 0.71073 Å). The crystals were cooled either slowly or rapidly to 100 K using an Oxford Instruments nitrogen cryostream or to 25 K using an Oxford Instruments helium cryostream.

Data collections were performed at various temperatures over the range 25 to 375 K. Data collection, integration of frame data and conversion to intensities corrected for Lorenz, polarization and absorption effects were performed using the programs SMART, SAINT+ and SADABS. Structure solutions, refinement of the structures, structure analyses and production of crystallographic illustrations were carried out using the programs SHELXS-97, SHELXL-97, WebLab Viewer Pro and ORTEP.

Physical Characterisation

Diffuse reflectance infrared Fourier transform spectra of single-crystal samples of **A1** and **A2** were collected on a BIO-RAD FTS-40 spectrophotometer with Win-IR Windows based software. CsI was used as the matrix and background over a range of 100 to 4000 cm^{-1}. The spectra indicated the similarity in the symmetry of the two compounds. Both compounds absorbed significantly in only

two regions, 450 cm^{-1} and 2210 cm^{-1}, energies characteristic of metal-cyanide and cyanide vibrations.

A solid state ultraviolet/visible reflectance spectrum of a single-crystal sample of **A1** was collected on a CARY 1E UV-Vis spectrophotometer equipped with custom designed Fourier transform analysis software. The spectrum indicated the optical transparency of the material.

Example 7 Synthesis and Characterisation

Synthesis

Single crystals of **B1** were prepared by slow diffusion of solutions of silver(I) nitrate into stoichiometric (2:1) solutions of potassium tetracyanozincate(II). Alternatively, polycrystalline samples of **B1** were prepared by diffusion of solutions of zinc(II) acetate into stoichiometric (1:2) solutions of potassium dicyanoargentate(I).

Large single crystals of **B2** were prepared by slow diffusion of solutions of zinc(II) acetate into stoichiometric (1:2) solutions of potassium dicyanoaurate(I). The diffusion techniques included:
(a) Test tubes, where an aqueous solution of one reagent was layered above an aqueous solution of the other reagent. Often a buffer region of pure solvent was introduced between the two solutions;
(b) U-shaped tubes, where the reagents diffused toward one another through a curved region beneath the initial position of the solutions.

Large colourless hexagonal prisms were grown by each of these techniques over time periods ranging from days (test-tubes) to weeks (U-tubes). Each single crystal was observed to be homochiral and bulk samples consisted of equal quantities of enantiomorphic crystals.

Structural Characterisation

Single crystals of **B1** and **B2** were mounted on a mohair fibre using a thin film of perfluoropolyether oil and transferred to a Bruker-AXS Smart 1000 CCD diffractometer equipped with Mo-Kα graphite monochromated radiation (lambda = 0.71073 Å). The crystals were cooled rapidly to 107 K using an Oxford Instruments nitrogen cryostream. Further data collections were performed at 150 K (**B2**) and 200 K (**B1**).

Data collection, integration of frame data and conversion to intensities corrected for Lorenz, polarization and absorption effects were performed using the programs SMART, SAINT+ and SADABS. Structure solutions, refinement of the structures, structure analyses and production of crystallographic illustrations were carried out using the programs SHELXS-97, SHELXL-97, WebLab Viewer Pro and ORTEP.

Example 8 Synthesis and Characterisation

Synthesis

Large single crystals of **C1** and **C2** were prepared by slow diffusion of solutions of cadmium(II) nitrate into stoichiometric (1:2) solutions of potassium dicyanoargentate(I) (**C1**) or potassium dicyanoaurate(I) (**C2**). Alternatively, single crystals of **C1** were obtained by slow diffusion of solutions of silver(I) nitrate into stoichiometric (2:1) solutions of potassium tetracyanocadmate(II). Both compounds were also prepared as bulk samples without need for slow diffusion. Inspection indicated the high degree of crystallinity present in samples prepared in this way.

Diffusion techniques (described above) included the use of (a) test tubes, where an aqueous solution of one reagent was layered above an aqueous solution of the other

reagent; often, a buffer region of pure solvent was introduced between the two solutions; (b) U-shaped tubes, where the reagents diffused toward one another through a curved region beneath the initial position of the solutions.

Large colourless triangular and hexagonal platelets were grown by each of these techniques over time periods ranging from days (test-tubes) to weeks (U-tubes).

Structural Characterisation

Single crystals of **C1** and **C2** were mounted on a mohair fibre using a thin film of perfluoropolyether oil and transferred to a Bruker-AXS Smart 1000 CCD diffractometer equipped with Mo-Kα graphite monochromated radiation (lambda = 0.71073 Å). The crystals were cooled rapidly to 107 K using an Oxford Instruments nitrogen cryostream. Data were also collected at 200 K. Data collection, integration of frame data and conversion to intensities corrected for Lorenz, polarization and absorption effects were performed using the programs SMART, SAINT+ and SADABS.

Structure solutions, refinement of the structures, structure analyses and production of crystallographic illustrations were carried out using the programs SHELXS-97, SHELXL-97, WebLab Viewer Pro and ORTEP.

Example 9 Synthesis and Characterisation

Synthesis

Large single crystals of **D** were prepared by slow diffusion of solutions of tetrakisacetonitrilocopper(I) tetrafluoroborate, zinc(II) acetate and tetramethylammonium haxafluorophosphate into stoichiometric solutions of potassium cyanide. Diffusion techniques included (a) test tubes, where an aqueous

solution of one reagent was layered above an aqueous solution of the other reagent; often a buffer region of pure solvent was introduced between the two solutions; (b) U-shaped tubes, where the reagents diffused toward one another through a curved region beneath the initial position of the solutions.

Colourless tetrahedra were grown by each of these techniques over time periods ranging from days (test-tubes) to weeks (U-tubes).

Structural Characterisation

A single crystal of **D** was mounted on a mohair fibre using a thin film of perfluoropolyether oil and transferred to a Bruker-AXS Smart 1000 CCD diffractometer equipped with Mo-Kα graphite monochromated radiation (lambda = 0.71073 Å). The crystal was cooled rapidly to 107 K using an Oxford Instruments nitrogen cryostream. Data were collected at 107 K and again at 200 K. Data collection, integration of frame data and conversion to intensities corrected for Lorenz, polarization and absorption effects were performed using the programs SMART, SAINT+ and SADABS. Structure solutions, refinement of the structures, structure analyses and production of crystallographic illustrations were carried out using the programs SHELXS-97, SHELXL-97, WebLab Viewer Pro and ORTEP.

Example 10 Synthesis and Characterisation

Synthesis

Large single crystals of **E1** and **E2** were prepared by slow diffusion of solutions of cadmium(II) nitrate into stoichiometric (1:1) solutions of potassium tetracyanonickelate(II) (**E1**) or potassium tetracyanoplatinate(II) (**E2**). Such diffusion techniques

included(a) test tubes, where an aqueous solution of one reagent was layered above an aqueous solution of the other reagent; often a buffer region of pure solvent was introduced between the two solutions;

(b) U-shaped tubes, where the reagents diffused toward one another through a curved region beneath the initial position of the solutions.

Colourless rods were grown by each of these techniques over time periods ranging from days (test-tubes) to weeks (U-tubes).

Structural Characterisation

Single crystals of **E1** and **E2** were mounted on a mohair fibre using a thin film of perfluoropolyether oil and transferred to a Bruker-AXS Smart 1000 CCD diffractometer equipped with Mo-Kα graphite monochromated radiation (lambda = 0.71073 Å). The crystals were cooled rapidly to 107 K using an Oxford Instruments nitrogen cryostream. Data were collected at 107 K and again at 150 K (**E1**) or 200 K (**E2**).

Data collection, integration of frame data and conversion to intensities corrected for Lorenz, polarization and absorption effects were performed using the programs SMART, SAINT+ and SADABS. Structure solutions, refinement of the structures, structure analyses and production of crystallographic illustrations were carried out using the programs SHELXS-97, SHELXL-97, WebLab Viewer Pro and ORTEP.

The anomalous thermal expansion properties exhibited by the materials described above were observed to arise from the thermal population of transverse vibrational modes of cyanide ion bridges, thermal population of rigid unit modes (RUMs), lattice effects and from conventional causes of NTE in non-cyanide containing materials. In

materials containing atoms bridged by cyanide ions, the most general cause of NTE was thermal population of the transverse vibrational modes.

The exact number and effect of these modes was also observed to depend on the geometry and symmetry of the cyanide bridge. However, at least one of the modes was observed to always contribute a negative component to the overall expansion properties of the materials. Other aspects which contributed to the overall thermal expansion properties of the materials included their composition, topology and whether or not ions or guest molecules were included therein.

Judicious choice of the appropriate parameters allowed for preparation of materials with a range of desired thermal expansion behaviours.

Explanation of Anomalous Thermal Behaviour in Cyanide-Containing Materials

The δ_1 and δ_2 transverse vibrational modes are illustrated in Figure 19 which depicts representations of the two transverse vibrational modes present in $Zn(CN)_2$ and similar systems with linear M-CN-M´ linkages. δ_1 involved the movement of the entire CN bridge away from the central M-M´ axis; δ_2 resembles a rotation of the CN bridge around an axis perpendicular to the central M-M´ axis. Both caused a decrease in the M-M´ distance.

The inventors noted that these vibrational modes both resulted in a net decrease of the M-M´ distance, which became more significant as the population of the modes was increased. The inventors discovered that these modes had sufficiently low energy that the negative contribution to the overall thermal expansion caused by population of these modes outweighed the positive contribution of the

stretching modes, and that this was responsible for NTE in the $Zn_xCd_{1-x}(CN)_2$ family.

The inventors also noted that when a material contained a number of M-CN-M´ linkages joined in a polymeric fashion (such as in $Zn(CN)_2$), vibrational modes were often coupled into lattice vibrations (known as rigid unit modes or RUMs), being forms of phonon modes. The term 'rigid unit' was used because these modes caused little to no distortion in the rigid polyhedra (such as the $[ZnC_xN_{4-x}]$ tetrahedra present in $Zn(CN)_2$). As such, they were typically of low energy, and hence were often more significantly populated than modes involving distortion or stretching of bond lengths (which could give rise to PTE). These RUMs were considered to be the manifestation of the above vibrational modes in a lattice, such that they also resulted in a net decrease in the M-M´ distance. A representation of two of the RUMs present in the $Zn(CN)_2$ lattice is given in Figure 20, which shows two of the rigid unit modes (RUMs) present in $Zn(CN)_2$.

In Figure 20, the zinc coordination spheres are illustrated as tetrahedra designated Zn; the cyanide linkages as rods designated CN. The first RUM (left) was a lattice vibration in which adjacent tetrahedra rotated in opposite directions; this corresponded to every M-CN-M´ link undergoing the δ_1 vibrational mode. The second RUM (right) is a lattice vibration in which all tetrahedra rotated in the same direction corresponded to the δ_2 vibrational mode. As for the individual vibrational modes, each of these lattice vibrations resulted in a decrease of the M-M´ distance.

The situation increased in complexity when the M-CN-M´ linkages deviated from the strictly linear ideal. Such systems often contained different vibrational modes, some

of which contributed to positive- rather than negative-thermal expansion. However, a mode similar to the δ_2 mode mentioned above was found to necessarily exist, and to contribute a negative component to the overall expansion behaviour of the material. Whether this and other NTE modes dominated over the PTE modes was sometimes difficult to predict and depended on the nature of each individual compound - its composition and structure.

The inventors also observed anomalous thermal expansion behaviour in some cyanide-containing materials (such as $Zn[Au(CN)_2]_2$) that appeared to arise not only from the above vibrational analysis, but also from lattice effects. Heating of these materials caused the geometry of the lattice itself to change, often resulting in uniaxial or anisotropic NTE. In addition to these effects, any of the causes of NTE in non-cyanide containing materials were also noted as potentially contributing an NTE component to appropriate CN-bridged compounds. Such phenomena were observed to include phase transitions, magnetic and electronic transitions and other (not necessarily CN-based) RUMs or phonon modes.

Any reference herein to a prior art document or use is not an admission that the document or use forms part of the common general knowledge of a skilled person in this field.

Whilst the invention has been described with reference to a number of preferred embodiments, it should be appreciated that the invention can be embodied in many other forms.

The Claims Defining the Invention are as follows:

1. A method for controlling the thermal expansion behaviour of a material comprising the step of incorporating into the material a component including one or more diatomic bridges, the or each bridge extending between two atoms in the component, characterised in that the or each diatomic bridge has at least one vibrational mode that causes the two atoms on either side of the bridge to be moved together to a greater extent than competing vibrational mode(s) that cause the two atoms on either side of the bridge to be moved apart.

2. A method as claimed in claim 1 wherein the component comprises a portion or the entirety of the material.

3. A method as claimed in claim 1 or 2 wherein the component comprises a portion of the material in an amount or manner that predetermines the material thermal expansion behaviour.

4. A method as claimed in any one of the preceding claims wherein the diatomic bridge has at least two vibrational modes δ_1 and δ_2 (as herein defined).

5. A method as claimed in any one of the preceding claims wherein, when the material includes a plurality of diatomic bridges throughout an infinite molecular coordination network defining a lattice structure, changes in lattice geometry induce material negative thermal expansion behaviour.

6. A method as claimed in any one of the preceding claims wherein the diatomic bridge is linear.

7. A method as claimed in any one of the preceding claims wherein the diatomic bridge is defined by a linear cyanide -(CN)- bridge.

8. A method as claimed in any one of claims 1 to 4 wherein the diatomic bridge is defined by a carbon monoxide -(CO)- bridge, a di-nitrogen -(NN)- bridge, a nitrogen monoxide -(NO)- bridge or a carbide -(CC)- bridge.

9. A method as claimed in any one of the preceding claims wherein the two atoms are metals or semi-metals.

10. A method as claimed in claim 9 wherein the diatomic bridge is a cyanide ion coordinated to the metal or semi-metal atoms, and one or both metal or semi-metal atoms in turn coordinates one or more other cyanide ions, which in turn bridge to other atoms.

11. A method as claimed in claim 10 wherein each atom alternatively coordinates other ligands.

12. A method as claimed in claim 11 wherein the other ligands are uni- or multi-dentate, including water, alcohols, diols, thiols, oxalate, nitrate, nitrite, sulfate, phosphate, oxide, sulfide, thiocyanate, non-bridging cyanide, cyanate, nitrogen monoxide, carbon monoxide, dinitrogen.

13. A method as claimed in claim 12 wherein the material is an optionally desolvated salt.

14. A method as claimed in claim 12 or 13 wherein the component forms part of an assembly that is neutrally, positively or negatively charged.

15. A method as claimed in claim 14 wherein when the assembly carries a charge, counter-ions are incorporated within cavities within the assembly to provide neutrally charged materials.

16. A method as claimed in claim 15 wherein the counter-ions influence the thermal behaviour of the material, and counteract negative expansion behaviour of the material.

17. A method as claimed in claims 15 or 16 wherein the material is porous.

18. A method as claimed in claim 17 wherein the counter-ions are included into pores of the material.

19. A method as claimed in any one of claims 15 to 18 wherein the counter-ions are varied either by ion exchange or synthetic modification, to vary the thermal behaviour of the material.

20. A method as claimed in any one of claims 12 to 19 wherein the material includes guest molecules located in interstitial cavities within a lattice thereof.

21. A method as claimed in claim 20 wherein the guest molecules influence the thermal behaviour and optionally counteract negative expansion behaviour of the material.

22. A method as claimed in claim 20 or 21 wherein the material is porous and the guest molecules are located in pores of the material.

23. A method as claimed in any one of claims 20 to 22 wherein the guest molecules are varied either by sorption/desorption or synthetic modification, to vary the thermal behaviour of the material.

24. A method as claimed in any one of claims 12 to 23 wherein the material has a topology based on a diamond-, wurzite-, quartz-, cubic-, (4,4)-, (6,3)-, (10,3)-, PtS-, NbO-, Ge_3N_4-, $ThSiO_2$- or PtO_x-type net.

25. A method as claimed in claim 24 wherein the material includes more than one interpenetrating net of the same or different topology.

26. A method as claimed in any one of the preceding claims wherein the material contains zero-dimensional bridged moieties, such as CN bridged molecular squares.

27. A method for controlling the thermal expansion behaviour of a material comprising the step of incorporating into the material a component including one or more multi-atomic bridges, the or each bridge extending

between two atoms in the material, characterised in that the or each multi-atomic bridge has at least one vibrational mode that causes the two atoms on either side of the bridge to be moved together to a greater extent than competing vibrational mode(s) that cause the two atoms on either side of the bridge to be moved apart.

28. A method as claimed in claim 27 wherein diatomic bridges as defined in any one of claims 4 to 12, or polyatomic bridges such as cyanamide, dicyanamide, tricyanomethanide, thiocyanate, selenocyanate, cyanate, isothiocyanate, isoselenocyanate, isocyanate, azide, cyanogen or butadyinide, are present in the component.

29. A method as claimed in claims 27 or 28 that is otherwise as defined in any one of claims 1 to 26.

30. A method for controlling the thermal expansion behaviour of a material substantially as herein described with reference to the Examples and/or the accompanying drawings.

31. A material produced by the method of any one of the preceding claims.

32. A material as claimed in claim 31 including one or more of:

(a) materials based on the $Zn(CN)_2$-type or 2x(6,4) cubic structure (doubly interpenetrating diamond nets), optionally including substitution of divalent metals for some or all of the Zn atoms, including Cd(II), Hg(II), Mn(II), Be(II), Mg(II), Pb(II) and Co(II), and optionally including substitution of mixtures of univalent, and optionally divalent and trivalent metal ions for Zn to give materials of the form: $\{(M1_1^{II})_{x1}(M1_2^{II})_{x2}...(M1_n^{II})_{xn}\}\{(M2_1^{I})(M3_1^{III})\}_{y1}\{(M2_2^{I})(M3_2^{III})\}_{y2}...\{(M2_m^{I})(M3_m^{III})\}_{ym}(CN)_2$ where $M1_i$ included Zn(II), Cd(II), Hg(II), Mn(II), Be(II), Mg(II), Pb(II) and Co(II); $M2_j$

includes Li(I) and Cu(I); $M3_k$ includes Al(III), Ga(III) and In(III); n and m being any non-negative whole numbers with at least one greater than or equal to unity; and (x1 + x2 +... +xn) + 2 x (y1 + y2 +... +ym) = 1;

(b) materials of (a) but with a single diamond-type network rather than two interpenetrating networks, optionally with other ions or molecules incorporated into the structure, optionally with the inclusion of lower- or higher-valent metals into the network lattice;

(c) materials of (a) and (b) but with more than two interpenetrating diamond networks;

(d) materials based on $Ga(CN)_3$-type structure, optionally satisfying the general formula:

$\{(M1_1^{III})_{x1}(M1_2^{III})_{x2}...(M1_n^{III})_{xn}\}\{(M2_1^{II})(M3_1^{IV})\}_{y1}\{(M2_2^{II})(M3_2^{IV})\}_{y2}...\{(M2_m^{II})(M3_m^{IV})\}_{ym}(CN)_3$ where M1 includes trivalent metal ions including Fe(III), Co(III), Cr(III), Ti(III), Al(III), Ir(III), Ga(III), In(III) and Sc(III); M2 includes divalent metal ions including Mg(II), Zn(II), Cd(II), Co(II), Fe(II), Ru(II), Mn(II) and Ni(II); M3 includes tetravalent metal ions such as Pd(IV) and Pt(IV); n and m being non-negative whole numbers with at least one greater than or equal to unity; and (x1 + x2 +... +xn) + 2 x (y1 + y2 + ... + ym) = 1;

(e) materials of (d) but with other ions or molecules being incorporated in the structure, including lower- or higher-valent metals in the network lattice;

(f) materials of (d) and (e) but with more than one interpenetrating cubic framework;

(g) other simple metal cyanides not explicitly belonging to (a) to (f) of the general form:

$(M1^{n1+})_{x1}(M2^{n2+})_{x2}...(Mk^{nk+})_{xk}(CN)_i(.\{guest\})$ where M1, M2 ... Mk were metals with oxidation states n1+, n2+ ... nk+ respectively; k and i were positive whole numbers; (x1 x n1) + (x2 x n2)

+ ... + (xk x nk) = i; and {guest}, when present, includes any solvent or molecular species such as water, alcohols, organic solvents or gas molecules, optionally including single or multiple interpenetrating regular nets including quartz, NbO, PtS, Ge_3N_4, (10,3), $ThSi_2$, PtO_x or wurtzite nets;

(h) materials of (g) but with other ions or molecules incorporated into the structure, including lower- or higher-valent metals in the network lattice;

(i) other materials not belonging to (a) to (g) comprising cyanide-bridged atoms, including cyanide-bridged materials in which the coordination spheres of some or all metal atoms include one or more non-cyanide bridges, including water, alcohols, diols, thiols, oxalate, nitrate, nitrite, sulfate, phosphate, oxide, sulfide, thiocyanate, (non-bridging) cyanide, cyanate, nitrogen monoxide, carbon monoxide or dinitrogen, optionally comprising regular nets, and optionally including interstitial ions or guest molecules;

(j) materials of (i) that comprise finite cyanide-bridged moieties, optionally comprising cyanide-bridged polyhedra, polygons or finite chains, optionally comprising branches and components unrelated or unconnected to the cyanide-bridged moieties;

(k) materials of (a) to (i) where chemical composition is varied within the one crystal/crystallite by variation of crystallisation conditions, including concentrations and temperatures during crystallisation; and

(l) amorphous materials or glasses based on any one of (a) to (k).

33. A material as claimed in claim 32 wherein:

* material (a) includes $Zn(CN)_2$, $Zn_{0.8}Cd_{0.2}(CN)_2$, $Cd(CN)_2$, $Mn(CN)_2$, $Zn_{0.5}Hg_{0.5}(CN)_2$, $Li_{0.5}Ga_{0.5}(CN)_2$ and $Cu_{0.5}Al_{0.5}(CN)_2$;

* material (b) includes $Cd(CN)_2.\frac{1}{2}CCl_4$ and $[NMe_4]_{0.5}[Cu^{I}_{0.5}Zn^{II}_{0.5}(CN)_2]$;

* material (d) includes $Ga^{III}(CN)_3$, $Co^{III}(CN)_3$, $Al^{III}(CN)_3$ and $Cd^{II}_{0.5}Pt^{IV}_{0.5}(CN)_3$;

* material (e) includes the Prussian blues compounds such as $K[Fe^{II}Fe^{III}(CN)_6].xH_2O$, and their analogues;

* material (g) includes $Ag^{I}CN$, $Au^{I}CN$, $Zn^{II}Ag^{I}_2(CN)_4$ and $Zn^{II}Au^{I}_2(CN)_4$;

* material (h) includes $KCd^{II}[Ag^{I}(CN)_2]_3$ and $KCd^{II}[Au^{I}(CN)_2]_3$;

* material (i) includes $Ni^{II}(CN)_2.xH_2O$, $Fe_4[Re_6Se_8(CN)_6]_3.36H_2O$, $Cd^{II}Ni^{II}(CN)_4.xH_2O$ and $Cd^{II}Pt^{II}(CN)_4.xH_2O$; and

* material (k) includes $Zn_xCd_{1-x}(CN)_2$.

34. A composite incorporating a material produced by the method of any one of claims 1 to 30.

35. A composite as claimed in claim 34 including two or more different materials, each produced by the method of any one of the claims 1 to 30, and optionally a binding agent for the materials.

36. A composite as claimed in claim 34 including a material produced by the method of any one of the claims 1 to 30 together with an unrelated material (as herein defined), and optionally a binding agent for the materials.

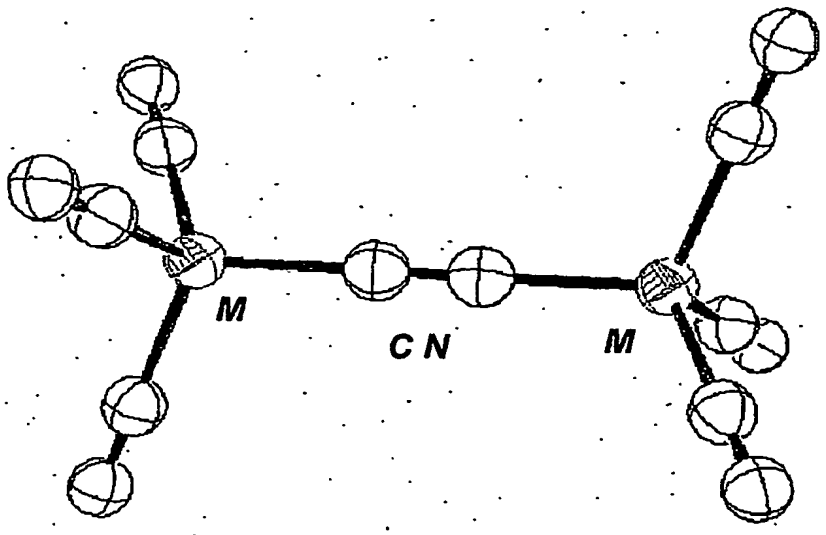

FIG. 1

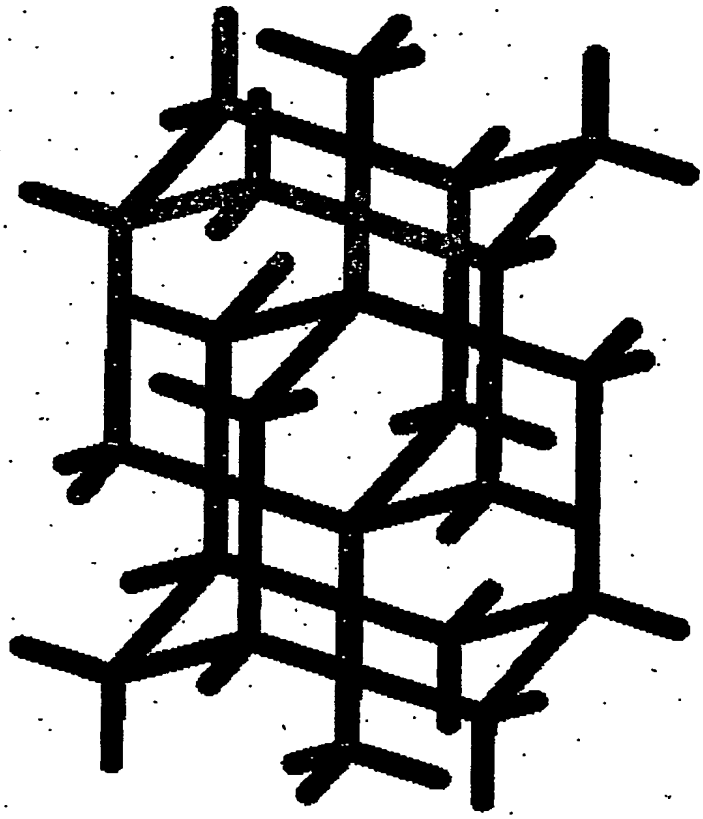

FIG. 2

(a)

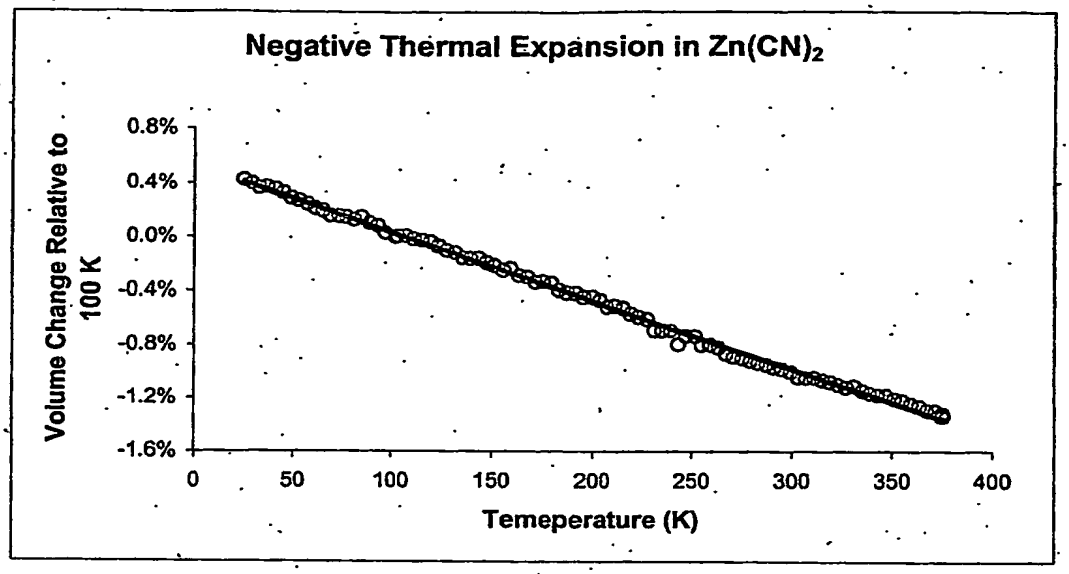
Negative Thermal Expansion in Zn(CN)2
Volume Change Relative to 100 K
0.8%
0.4%
0.0%
-0.4%
-0.8%
-1.2%
-1.6%
0
50
100
150
200
250
300
350
400
Temeperature (K)

(b)

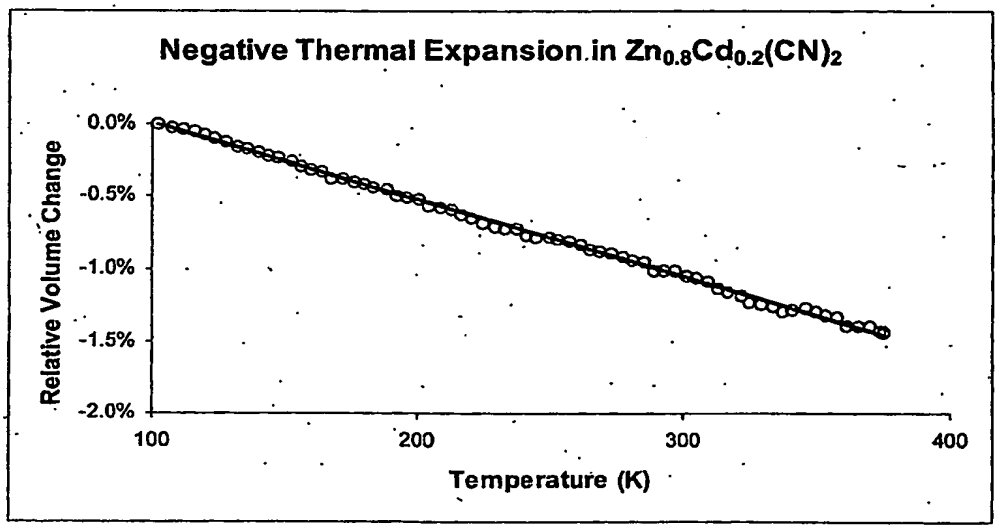
Negative Thermal Expansion in Zn0.8Cd0.2(CN)2
Relative Volume Change
0.0%
-0.5%
-1.0%
-1.5%
-2.0%
100
200
300
400
Temperature (K)

FIG. 3

(c)

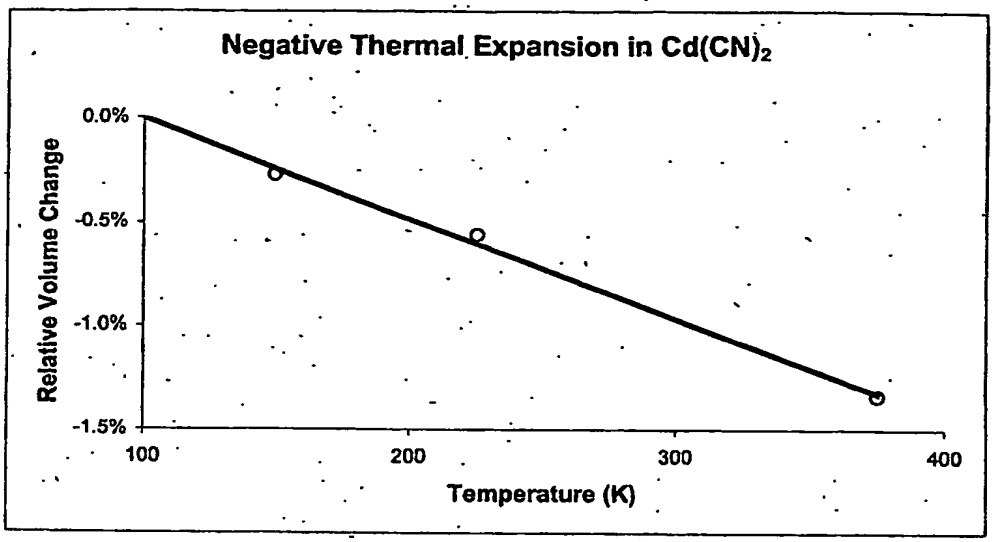
Negative Thermal Expansion in Cd(CN)2
Relative Volume Change
0.0%
-0.5%
-1.0%
-1.5%
100
200
300
400
Temperature (K)

FIG. 3

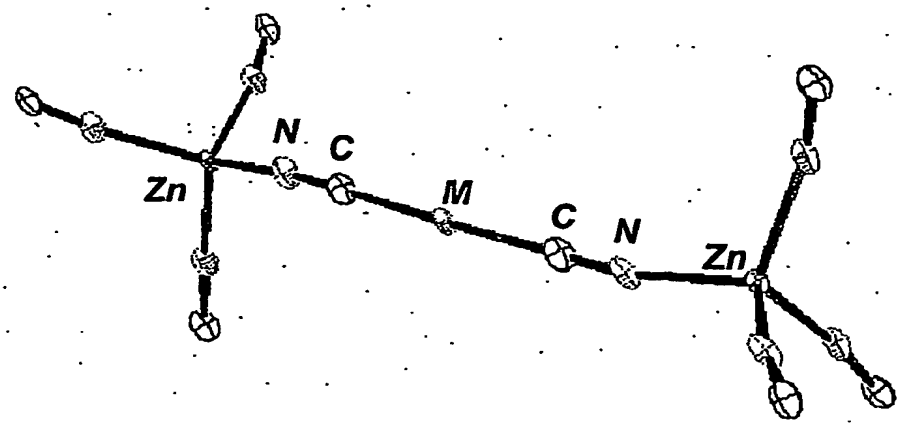

FIG. 4

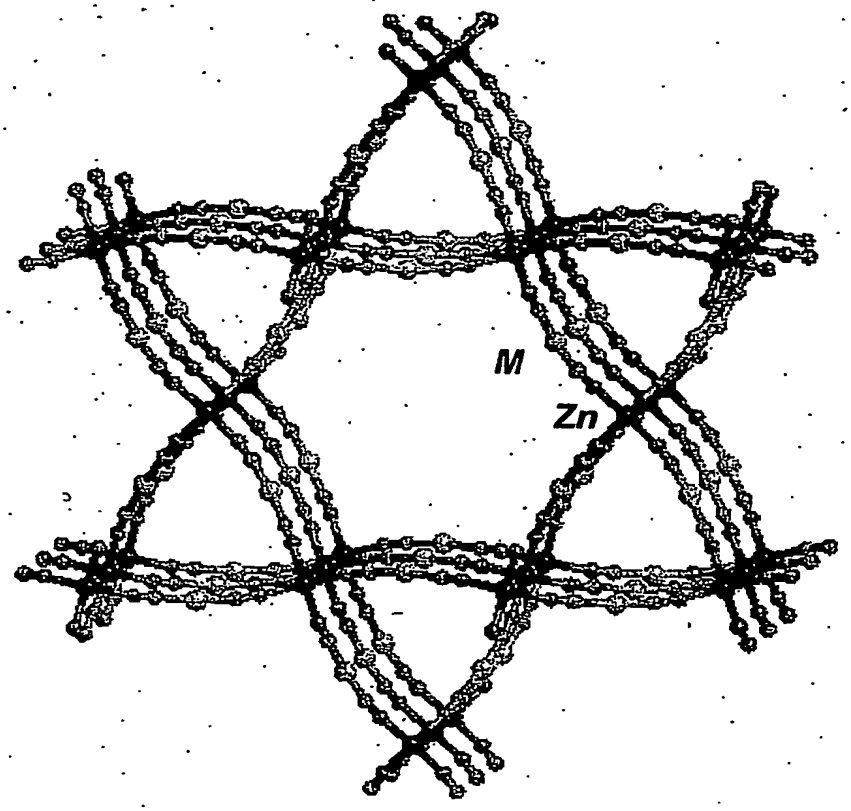

FIG. 5

(a)

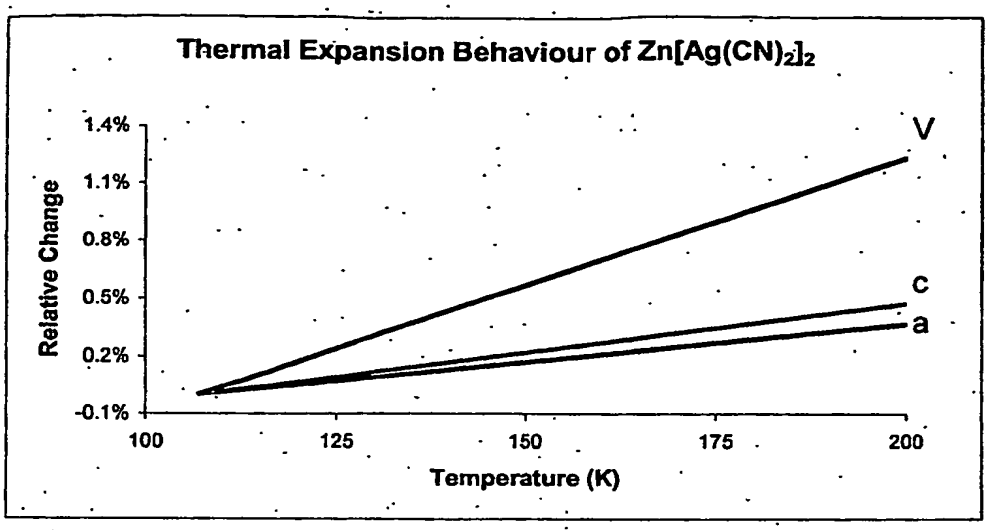
Thermal Expansion Behaviour of Zn[Ag(CN)2]2
Relative Change
1.4%
1.1%
0.8%
0.5%
0.2%
-0.1%
100
125
150
175
200
Temperature (K)
V
c
a

(b)

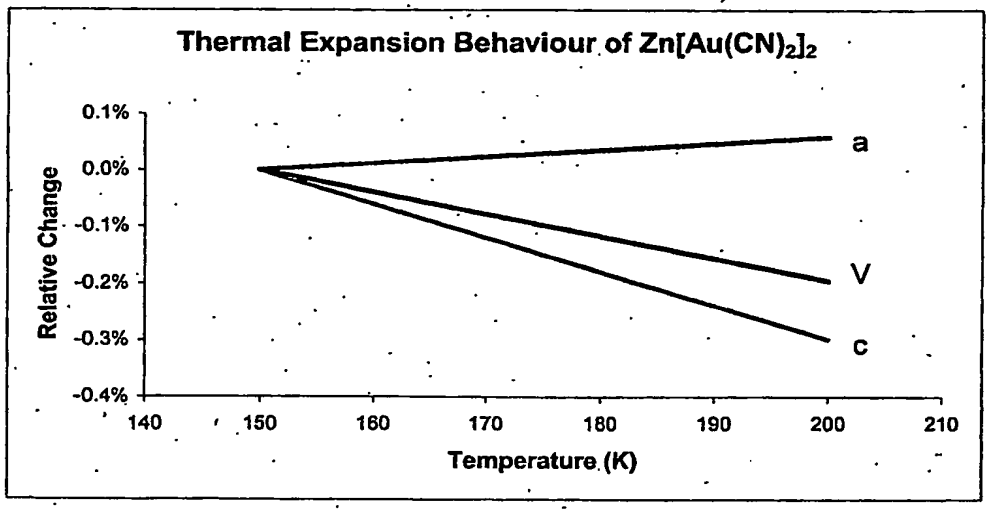
Thermal Expansion Behaviour of Zn[Au(CN)2]2
Relative Change
0.1%
0.0%
-0.1%
-0.2%
-0.3%
-0.4%
140
150
160
170
180
190
200
210
Temperature (K)
a
V
c

FIG. 6

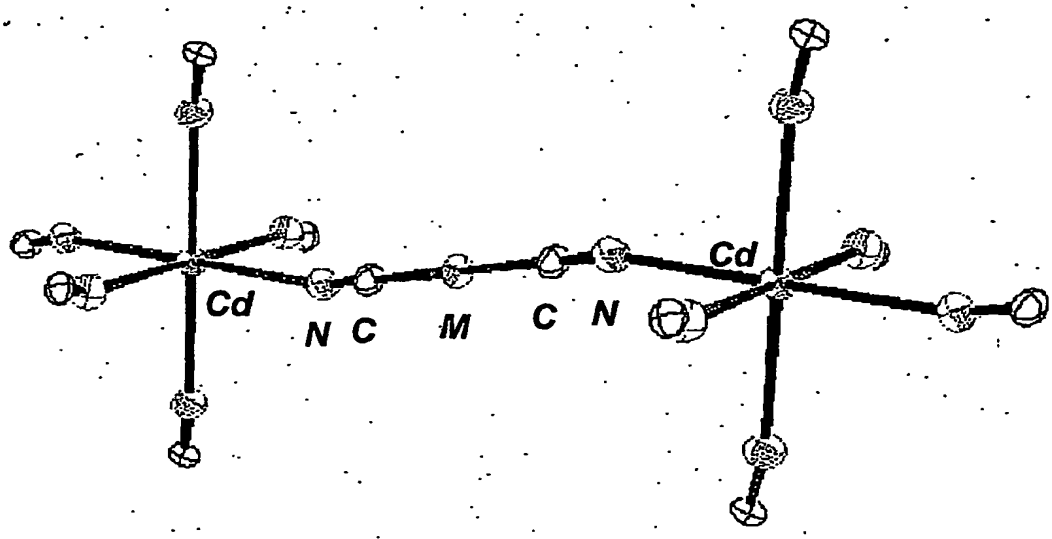

FIG. 7

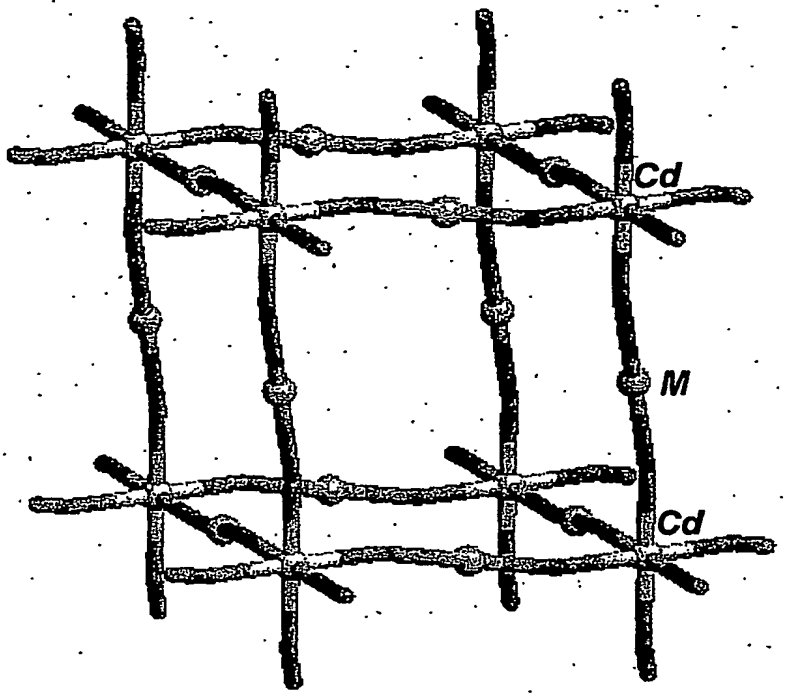

FIG. 8

(a)

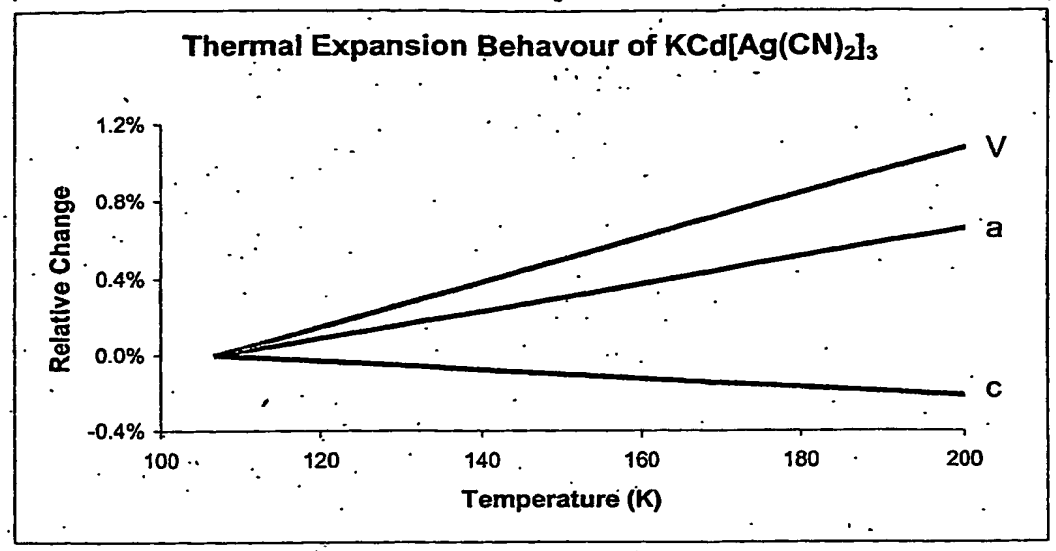
Thermal Expansion Behavour of KCd[Ag(CN)2]3
Relative Change
1.2%
0.8%
0.4%
0.0%
-0.4%
100
120
140
160
180
200
Temperature (K)
V
a
c

(b)

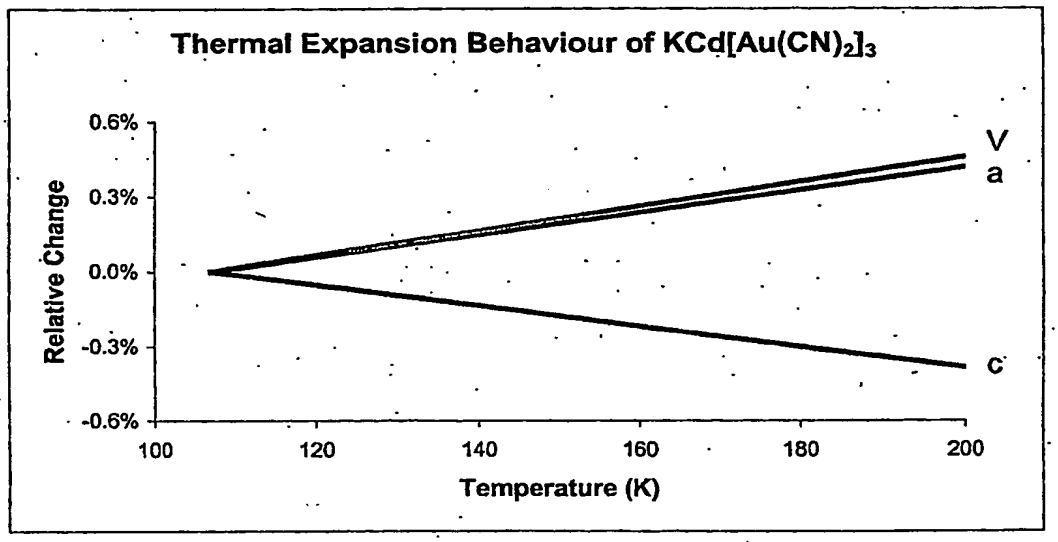
Thermal Expansion Behaviour of KCd[Au(CN)2]3
Relative Change
0.6%
0.3%
0.0%
-0.3%
-0.6%
100
120
140
160
180
200
Temperature (K)
V
a
c

FIG. 9

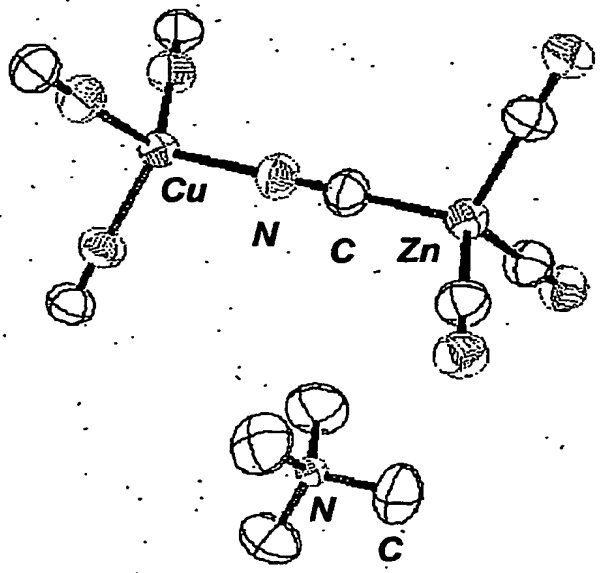

FIG. 10

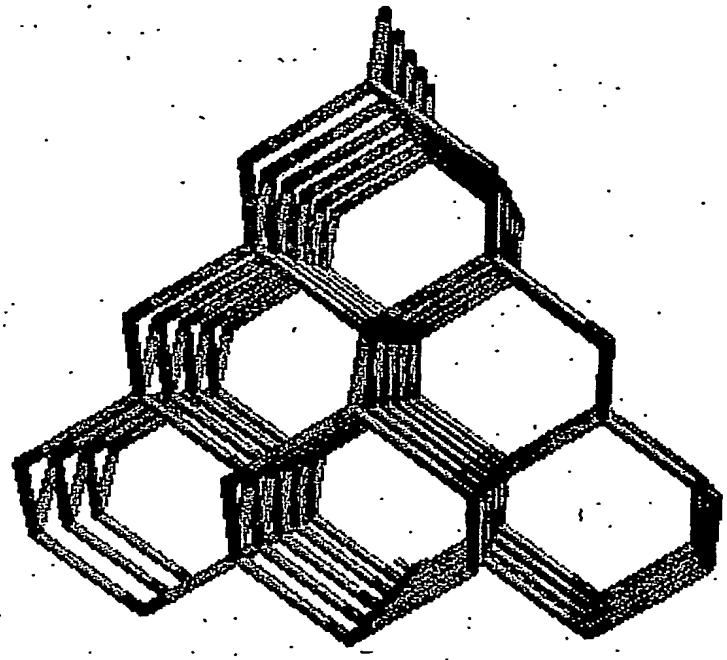

FIG. 11

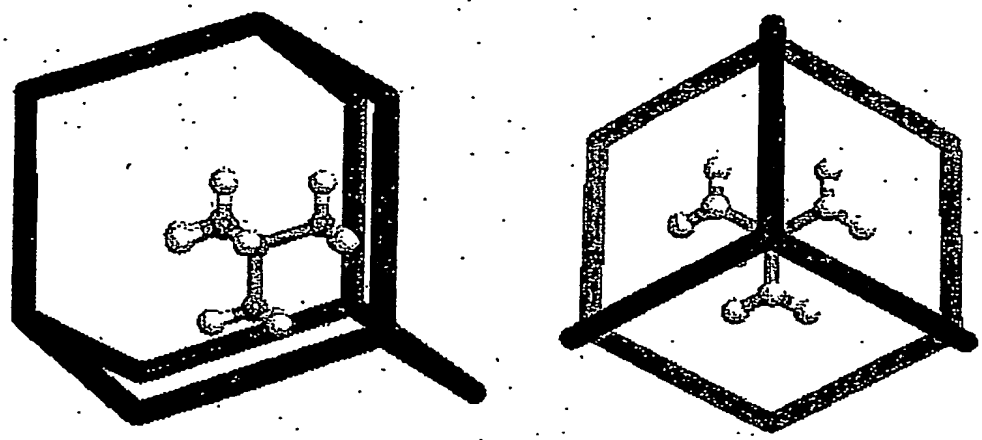

FIG. 12

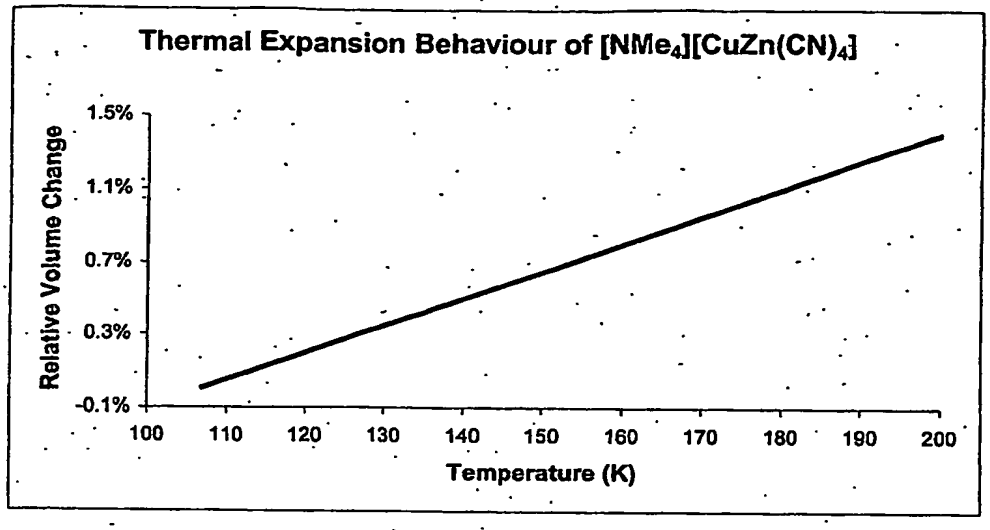
Thermal Expansion Behaviour of [NMe4][CuZn(CN)4]
Relative Volume Change
1.5%
1.1%
0.7%
0.3%
-0.1%
100
110
120
130
140
150
160
170
180
190
200
Temperature (K)

FIG. 13

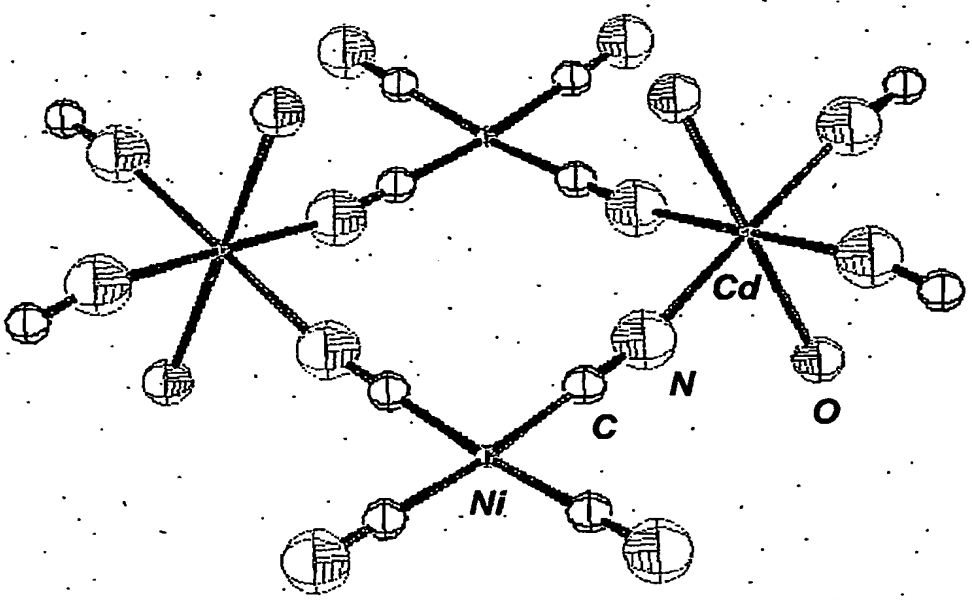

FIG. 14

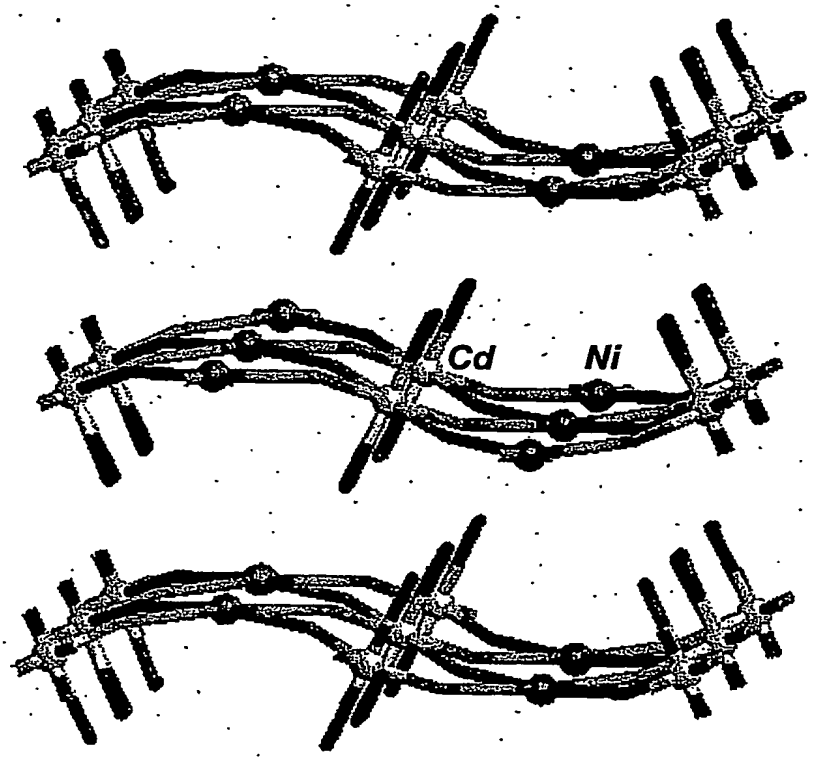

FIG. 15

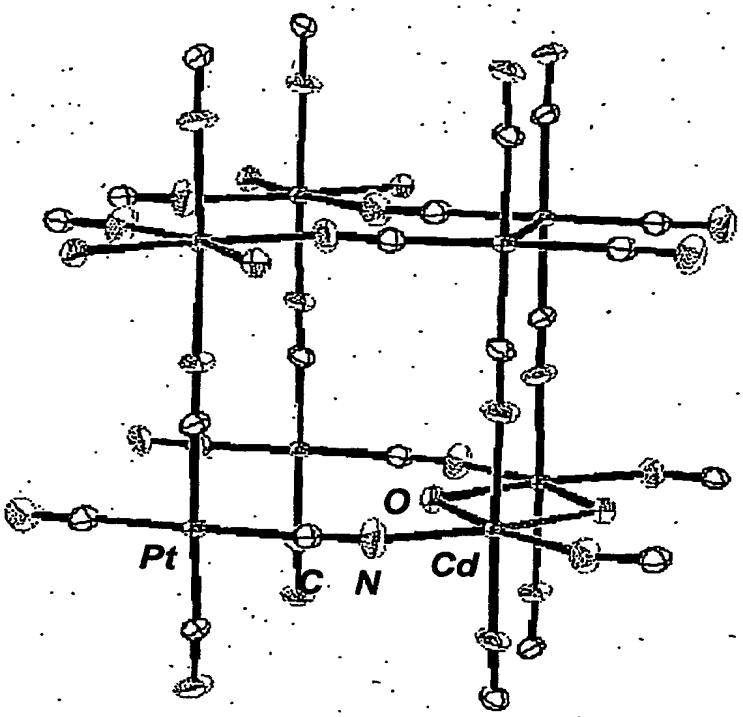

FIG. 16

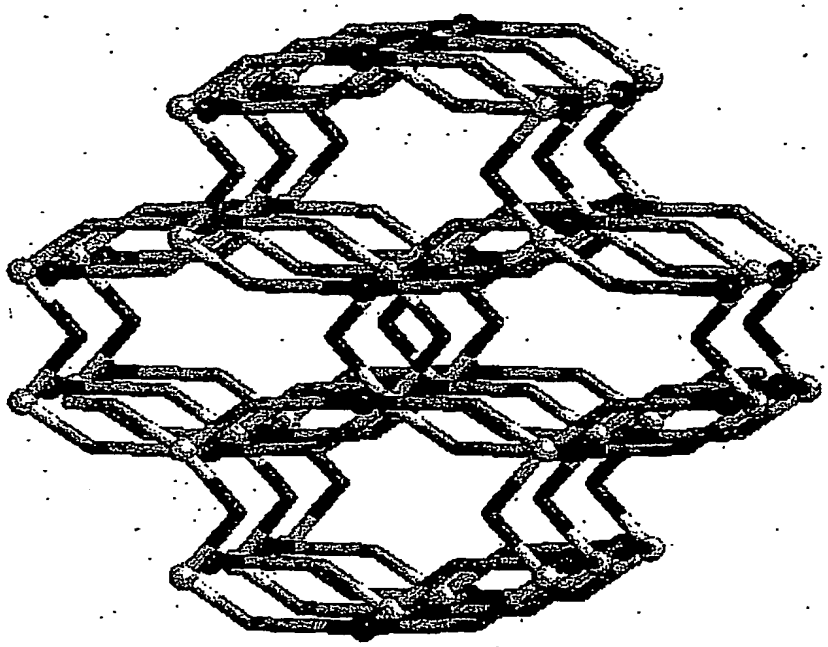

FIG. 17

(a)

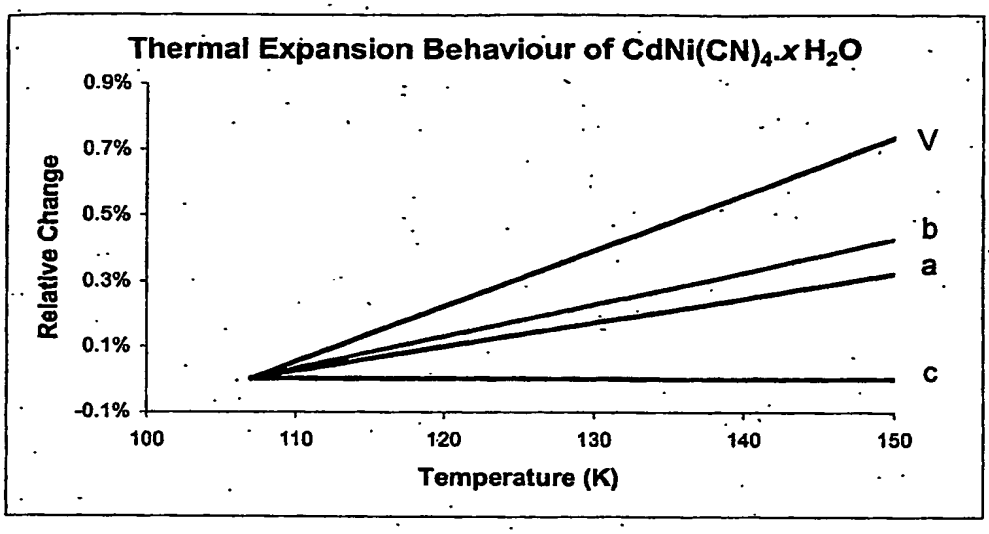
Thermal Expansion Behaviour of $CdNi(CN)_4.x\,H_2O$
Relative Change
0.9%
0.7%
0.5%
0.3%
0.1%
-0.1%
100
110
120
130
140
150
Temperature (K)
V
b
a
c

(b)

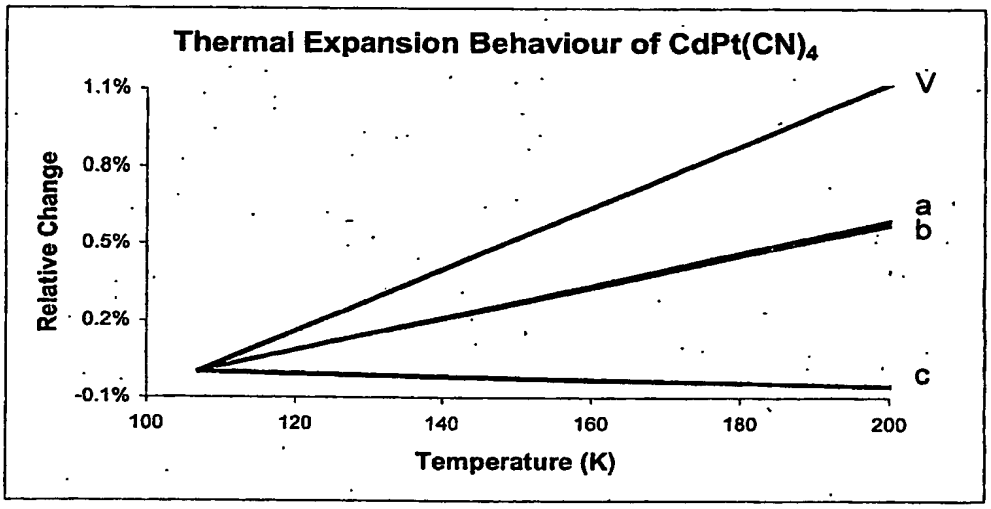
Thermal Expansion Behaviour of $CdPt(CN)_4$
Relative Change
1.1%
0.8%
0.5%
0.2%
-0.1%
100
120
140
160
180
200
Temperature (K)
V
a
b
c

FIG. 18

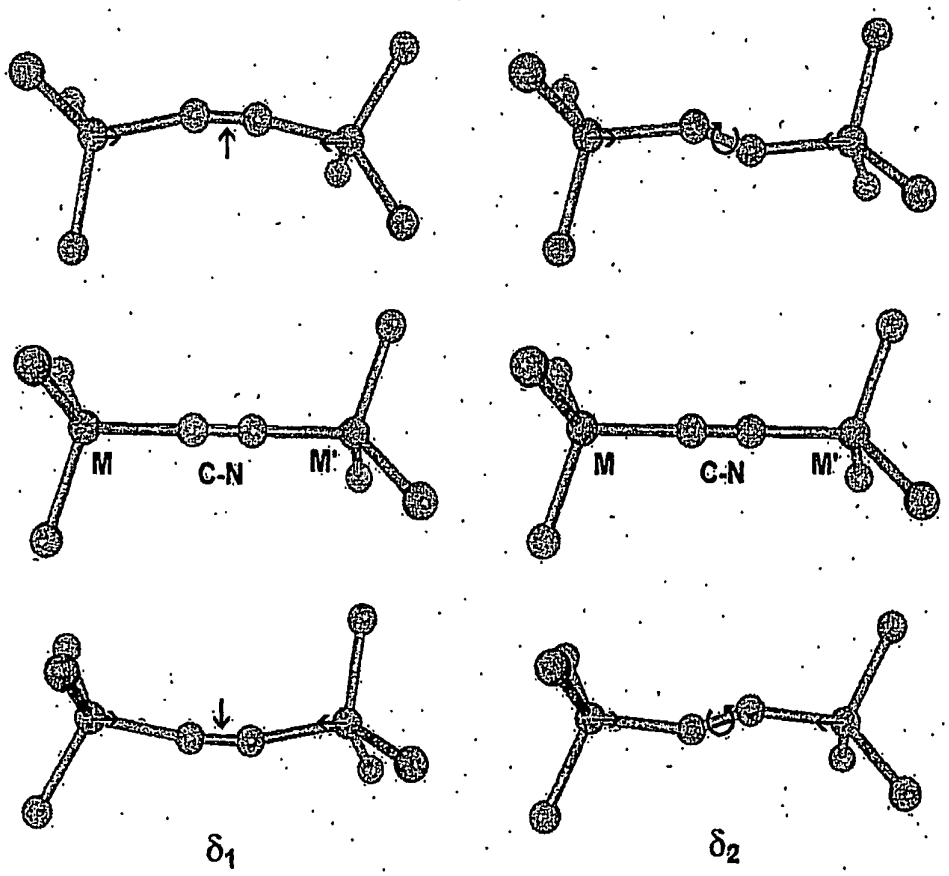

FIG. 19

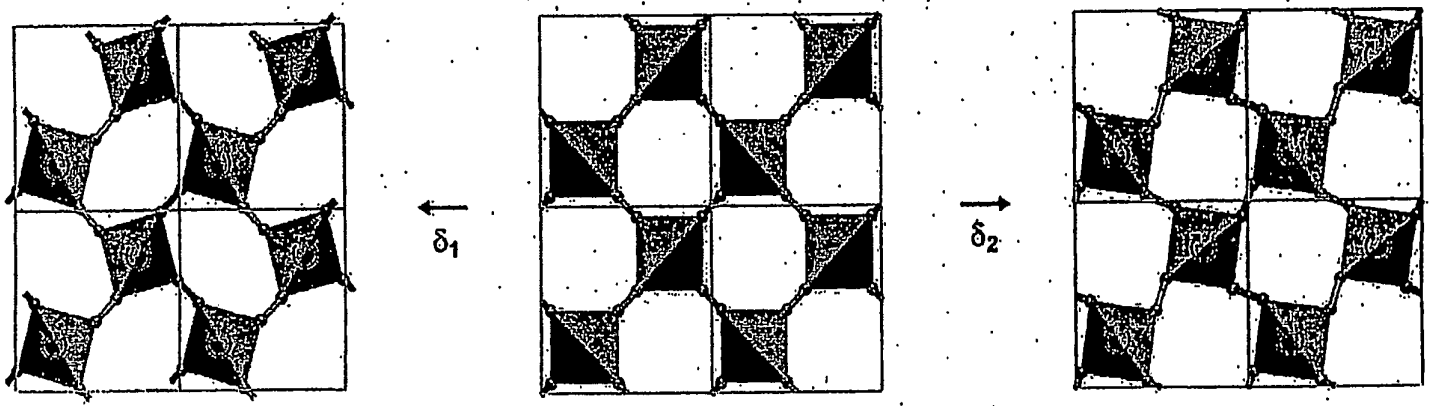

FIG. 20

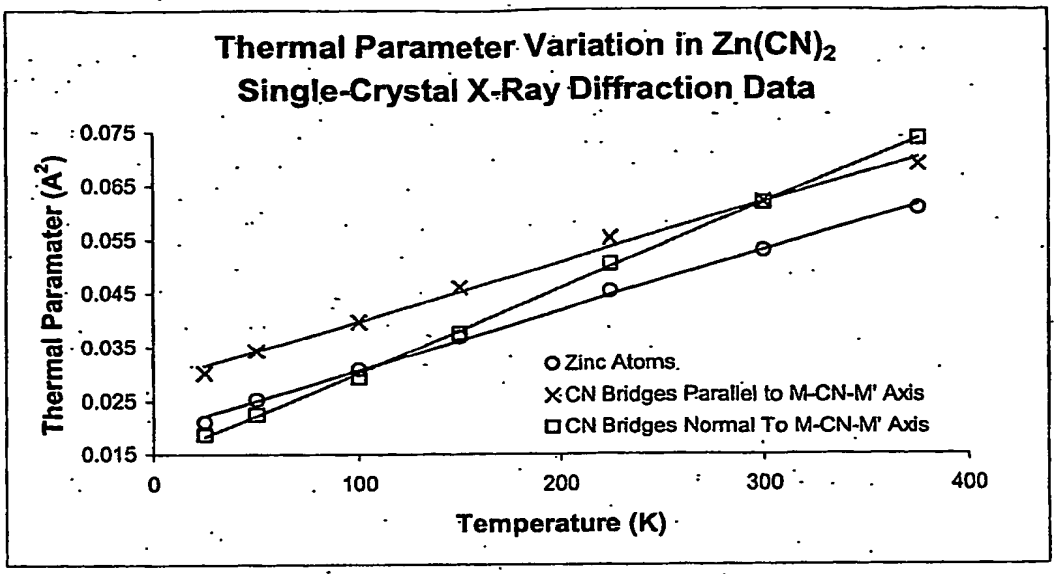
Thermal Parameter Variation in Zn(CN)2
Single-Crystal X-Ray Diffraction Data
Thermal Paramater (A2)
0.075
0.065
0.055
0.045
0.035
0.025
0.015
0
100
200
300
400
Temperature (K)
Zinc Atoms.
CN Bridges Parallel to M-CN-M' Axis
CN Bridges Normal To M-CN-M' Axis

FIG. 21